



Emergence of Coherent Localized Structures in Shear Deformations of Temperature Dependent Fluids

Theodoros Katsaounis, Julier Olivier, Athanasios Tzavaras

► To cite this version:

Theodoros Katsaounis, Julier Olivier, Athanasios Tzavaras. Emergence of Coherent Localized Structures in Shear Deformations of Temperature Dependent Fluids. 2014. hal-01087298

HAL Id: hal-01087298

<https://hal.science/hal-01087298>

Preprint submitted on 25 Nov 2014

HAL is a multi-disciplinary open access archive for the deposit and dissemination of scientific research documents, whether they are published or not. The documents may come from teaching and research institutions in France or abroad, or from public or private research centers.

L'archive ouverte pluridisciplinaire **HAL**, est destinée au dépôt et à la diffusion de documents scientifiques de niveau recherche, publiés ou non, émanant des établissements d'enseignement et de recherche français ou étrangers, des laboratoires publics ou privés.

EMERGENCE OF COHERENT LOCALIZED STRUCTURES IN SHEAR DEFORMATIONS OF TEMPERATURE DEPENDENT FLUIDS *

THEODOROS KATSAOUNIS^{1,2}, JULIER OLIVIER³, AND ATHANASIOS E. TZAVARAS⁴

ABSTRACT. Shear localization occurs in various instances of material instability in solid mechanics and is typically associated with Hadamard-instability for an underlying model. While Hadamard instability indicates the catastrophic growth of oscillations around a mean state, it does not by itself explain the formation of coherent structures typically observed in localization. The latter is a nonlinear effect and its analysis is the main objective of this article. We consider a model that captures the main mechanisms observed in high strain-rate deformation of metals, and describes shear motions of temperature dependent non-Newtonian fluids. For a special dependence of the viscosity on the temperature, we carry out a linearized stability analysis around a base state of uniform shearing solutions, and quantitatively assess the effects of the various mechanisms affecting the problem: thermal softening, momentum diffusion and thermal diffusion. Then, we turn to the nonlinear model, and construct localized states - in the form of similarity solutions - that emerge as coherent structures in the localization process. This justifies a scenario for localization that is proposed on the basis of asymptotic analysis in [10].

1. INTRODUCTION

The phenomenon of shear localization during high strain-rate deformations of metals [22, 3, 8] is a striking instance of material instability in mechanics, that has attracted considerable attention in the mechanics literature (*e.g.* [3, 7, 12, 19, 21]) as well as a number of mathematical studies ([4, 15, 2, 20, 17, 5, 10] and references therein). Material instability is typically associated with ill-posedness of an underlying initial value problem, what has coined the term *Hadamard instability* for its description in the mechanics literature. It should however be emphasized that while Hadamard instability indicates the catastrophic growth of oscillations around a mean state, what is observed in localization is the orderly albeit extremely fast development of coherent structures: the shear bands. The latter is a nonlinear phenomenon and a linearized analysis can only serve as a precursor to such behavior.

We work with the simplest model capturing the mechanism of shear band formation, a simple shear motion of a non-Newtonian fluid with temperature decreasing viscosity $\mu'(\theta) < 0$,

$$(1.1) \quad \begin{aligned} v_t &= \sigma_x, \\ \theta_t &= \kappa \theta_{xx} + \sigma v_x \\ \sigma &= \mu(\theta) v_x^n, \end{aligned}$$

¹ DEPARTMENT OF MATHEMATICS AND APPLIED MATHEMATICS, UNIVERSITY OF CRETE, HERAKLION, 71003, GREECE. EMAIL: thodoros.katsaounis@uoc.gr

² INSTITUTE OF APPLIED AND COMPUTATIONAL MATHEMATICS, FORTH, HERAKLION 71110, GREECE

³ CENTRE DE MATHÉMATIQUES ET INFORMATIQUE, AIX-MARSEILLE UNIVERSITÉ, 39 RUE F. JOLIOT CURIE, 13453 MARSEILLE CEDEX 13, FRANCE. EMAIL: julien.olivier@univ-amu.fr

⁴ COMPUTER, ELECTRICAL, MATHEMATICAL SCIENCES & ENGINEERING DIVISION, KING ABDULLAH UNIVERSITY OF SCIENCE AND TECHNOLOGY (KAUST), THUWAL, SAUDI ARABIA. EMAIL: athanasios.tzavaras@kaust.edu.sa

*Research partially supported by the EU FP7-REGPOT project “Archimedes Center for Modeling, Analysis and Computation” and the “Aristeia” program of the Greek Secretariat of Research. Part of this work was completed at the Institute of Applied and Computational Mathematics, FORTH, Greece.

where $n > 0$ describes the strain-rate sensitivity which typically in these problems satisfies $n \ll 1$. Mathematical studies of (2.1), for power law viscosities $\mu(\theta) = \theta^{-\alpha}$, $\alpha > 0$, show that the uniform shear is asymptotically stable for $n > \alpha$ [4, 15], but indicate unstable response in the complementary region $n < \alpha$, [15, 2, 17]. The mathematical analysis has not so far characterized the precise behavior in the instability region; however, detailed and resolved numerical studies (*e.g.* [19, 6, 1]) show that instability is followed by formation of shear bands.

The difficulty is that in order to analyze the unstable regime one needs to account for the combined effect of parabolic regularizations in conjunction to ill-posed initial value problems. An asymptotic theory for calculating an effective equation for the compound effect is proposed in [10, 11]. It is based on the theory of relaxation systems and the Chapman-Enskog expansion and produces an effective asymptotic equation. For a power law the effective equation changes type from forward to backward parabolic, across the threshold $-\alpha + n = 0$ of the parameter space. The criteria of [10, 11] are based on asymptotic analysis and as such are formal in nature.

Our objective, here, is to develop a mathematical theory for the onset of localisation and the emergence of a nonlinear localized state, thus providing a rigorous justification to the behavior conjectured by the effective equation in [10]. We employ the constitutive hypothesis of an *exponential law* for the viscosity coefficient,

$$(H_{exp}) \quad \mu(\theta) = e^{-\alpha\theta}, \quad \alpha > 0 \quad \text{and hence} \quad \sigma = e^{-\alpha\theta} v_x^n.$$

The model (2.1) for the exponential law (H_{exp}) admits a special class of solutions describing uniform shearing

$$(1.2) \quad \begin{aligned} v_s(x) &= x, \\ \theta_s(t) &= \frac{1}{\alpha} \log(\alpha t + c_0), \quad c_0 = e^{\alpha\theta_0}, \\ \sigma_s(t) &= \frac{1}{\alpha t + c_0}. \end{aligned}$$

The graph $\sigma_s - t$ describing the average stress vs. average strain response is monotonically decreasing, and thus the deformation of uniform shear is characterized by strain softening response. We set the following goals:

- (i) To study the linearized problem around the uniform shearing solution and to assess the effects of the various parameters of the problem
- (ii) To inquire whether there are special solutions of the nonlinear problem that indicate the emergence of localized deformations and formation of shear bands.

Since the base solution (1.2) around which we linearize is time-dependent the linearized analysis necessarily involves analysis of non-autonomous systems and also perturbations have to be compared against the base solution. We perform a linearization using ideas of relative perturbations

$$(1.3) \quad \begin{aligned} u &:= v_x = 1 + \delta \bar{u}(x, t) + O(\delta^2) \\ \theta &= \theta_s(t) + \delta \bar{\theta}(x, t) + O(\delta^2) \\ \sigma &= \sigma_s(t) + \delta \sigma_s(t) \bar{\sigma}(x, t) + O(\delta^2) \end{aligned}$$

leading to linearized system

$$(1.4) \quad \begin{cases} \bar{u}_t &= \sigma_s(t) (n \bar{u}_{xx} - \alpha \bar{\theta}_{xx}) \\ \bar{\theta}_t - \kappa \bar{\theta}_{xx} &= \sigma_s(t) ((n+1) \bar{u} - \alpha \bar{\theta}) \\ \bar{u}_x(0, t) = \bar{u}_x(1, t) &= 0, \\ \bar{\theta}_x(0, t) = \bar{\theta}_x(1, t) &= 0. \end{cases}$$

with $\bar{\sigma}$ computed by $\bar{\sigma} = n \bar{u} - \alpha \bar{\theta}$. This problem turns out to have the following behavior:

- (a) For the case without thermal diffusion $\kappa = 0$:

When $n = 0$ the high frequency modes grow exponentially fast with the exponent of the order of the frequency what is characteristic of ill-posedness and *Hadamard instability*.

When $n > 0$ the modes are still unstable but the rate of growth is bounded independently of the frequency. In fact, the behavior in that range is characteristic of *Turing instability*.

- (b) The effect of thermal diffusion ($\kappa > 0$) for the non-autonomous linearized model (1.4) can also be assessed: Perturbations do grow initially in the early stages of deformation, but over time the effect of the diffusion intensifies and eventually the system gets stabilized. For a quantitative description of the above qualitative statement we refer to lemmas 3.2 and 3.3. In addition, this behavior can also occur for the full solution of the nonlinear problem (1.1) subject to simple shear boundary conditions as indicated in numerical simulations presented in Figure 2. This type of metastable response was already conjectured (for a somewhat different model) in numerical experiments of [19, 18]. The linearized analysis presented here offers a theoretical explanation of this interesting behavior.

In the second part of this article we consider the adiabatic variant of the model (1.1) with exponential constitutive law (H_{exp}). The system is expressed for $u = v_x$ in the form

$$(1.5) \quad \begin{aligned} u_t &= \partial_{xx} \left(e^{-\alpha\theta} u^n \right) \\ \theta_t &= e^{-\alpha\theta} u^{n+1} \end{aligned}$$

and is now considered on the whole space $(x, t) \in \mathbb{R} \times [0, \infty)$. For the system (1.5), we construct a class of localizing solutions

$$(1.6) \quad \begin{aligned} u(x, t) &= \phi_\lambda(t) U_\lambda(\sqrt{\lambda}x\phi_\lambda(t)) \\ \sigma(x, t) &= \sigma_s(t) \frac{1}{\phi_\lambda(t)} \Sigma_\lambda(\sqrt{\lambda}x\phi_\lambda(t)) \\ \theta(x, t) &= \theta_s(t) + \lambda^{\frac{n+1}{\alpha}} (\theta_s(t) - \theta_0) + \Theta_\lambda(\sqrt{\lambda}x\phi_\lambda(t)) \end{aligned}$$

where $\phi_\lambda(t) = \left(\frac{\alpha}{c_0}t + 1\right)^{\frac{\lambda}{\alpha}}$ depends on the parameter $\lambda > 0$, and (1.6) is determined via the solution $(U_\lambda, \Sigma_\lambda, \Theta_\lambda)$ of the singular initial value problem (5.1), (5.2) with $\nu = \lambda$. The existence of the solution $(U_\lambda, \Sigma_\lambda, \Theta_\lambda)$ is established in Theorem 5.1 where most importantly its behavior at the origin and at infinity is precised. The emerging solution (1.6) depends on three parameters: θ_0 linked to the uniform shear in (1.2), a parameter λ which can be viewed as a length scale of initial data, and a Σ_0 determining the size of the initial profile.

To our knowledge this is the first instance that the compound effect of Hadamard instability and parabolic regularizations is mathematically analyzed in a nonlinear context. The reader should contrast the nonlinear response captured by the exact solution (1.6) to the response of the associated linearized problem (1.4). As precised in Theorem 6.1, the response of (1.6) indicates that the competition among Hadamard instability and momentum diffusion in a nonlinear context can lead to a nonlinear coherent structure that localizes in a narrow band. By contrast, for a linear model, the combined effect of Hadamard instability and parabolicity leads to unstable oscillatory modes growing in amplitude (see (3.22)). This justifies the scenario that nonlinearity can kill the oscillations caused by Hadamard instability so that the nonuniformity of deformation produced by the instability merges into a single localized zone. It would be interesting to explore this type of response for other models related to material instability in solid mechanics.

The exposition is organized as follows: Section 2 presents a description of the problem and the formulation via relative perturbations. The linearized analysis is presented in section 3, first the part that can be done via spectral analysis for autonomous systems, and then the part concerning

the effect of thermal diffusion, which is based on energy estimates for a non-autonomous linear system. Detailed asymptotics for the eigenvalues and the connection with Hadamard and Turing instabilities are presented there. The presentation of the localized solutions is split in sections 4-6: Section 4 presents the invariance properties, the *ansatz* of localized solutions, and also introduces the relevant auxiliary problem (5.1), (5.2). The construction of solutions to the singular initial-value problem (5.1), (5.2) and the proof of their properties is the centerpiece of our analysis and forms the objective of section 5. The construction is based on a series of steps, involving desingularization, a nonlinear transformation, and eventually the existence of a heteroclinic orbit via the Poincaré-Bendixson theorem. The construction of the localized solutions is then effected in section 6.

2. MODELING OF SHEAR BANDS - RELATIVE PERTURBATIONS

In this work we study the onset of localization and formation of shear bands for the model (1.1) describing shear motions of a non-Newtonian fluid with viscosity $\mu(\theta)$ decreasing with temperature. For concreteness we take a viscosity satisfying the exponential law (H_{exp}) and are interested in the range where the rate sensitivity n is positive and small. The model (1.1) then becomes

$$(2.1) \quad \begin{aligned} v_t &= \sigma_x, \\ \theta_t &= \kappa \theta_{xx} + \sigma v_x \\ \sigma &= e^{-\alpha \theta} v_x^n. \end{aligned}$$

and describes shear motions between two parallel plates located at $x = 0$ and $x = 1$ with v the velocity in the shear direction, σ the shear stress, θ the temperature, and

$$(2.2) \quad u = v_x$$

depicting the strain rate. The boundary conditions are taken

$$(2.3) \quad v(0, t) = 0, \quad v(1, t) = 1,$$

$$(2.4) \quad \theta_x(0, t) = 0, \quad \theta_x(1, t) = 0.$$

Equation (2.3) reflects prescribed velocities at the boundaries, while (2.4) manifests that the bounding plates are adiabatic. Note that (2.3) implies that the stress satisfies

$$(2.5) \quad \sigma_x(0, t) = \sigma_x(1, t) = 0,$$

and that

$$(2.6) \quad \int_0^1 u(x, t) dx = 1.$$

The initial conditions are

$$(2.7) \quad \begin{aligned} v(x, 0) &= v_0(x), \\ \theta(x, 0) &= \theta_0(x). \end{aligned}$$

Throughout the study we will consider two cases: When $\kappa = 0$ the process is adiabatic and the resulting model will be the main object of study, as it is the simplest model proposed for studying the phenomenon of formation of shear bands. The case $\kappa > 0$ will also be studied in section 3 as a paradigm to assess the effect of thermal diffusion.

2.1. Uniform shearing solutions. The problem (2.1), (2.3), (2.4) admits a class of special solutions describing uniform shear

$$\begin{aligned}
 (2.8) \quad & v_s = x, \\
 & u_s = \partial_x v_s = 1 \\
 & \theta_s = \theta_s(t) \\
 & \sigma_s = \sigma_s(t) = \mu(\theta_s(t)) \\
 (2.9) \quad & \text{with } \theta_s \text{ defined by } \begin{cases} \frac{d\theta_s}{dt} = \mu(\theta_s) = \sigma_s \\ \theta_s(0) = \theta_0 \end{cases}
 \end{aligned}$$

For the special case of the exponential law (H_{exp}), θ_s and σ_s read

$$\begin{aligned}
 (2.10) \quad & \theta_s = \frac{1}{\alpha} \log(\alpha t + c_0), \quad c_0 = e^{\alpha \theta_0}, \\
 & \sigma_s = \frac{1}{\alpha t + c_0}.
 \end{aligned}$$

These are universal solutions, *i.e.* they hold for all values of the parameters n, α, κ in the model (2.1) including the limiting elliptic initial value problem when $n = 0, \kappa = 0$. The graph $\sigma - t$ is viewed as describing the stress vs. average strain response. As the graph is decreasing, it means that there is always softening response in the course of the deformation.

2.2. Description of the phenomenon of shear bands. The system (2.1) has served as a paradigm for the mathematical study of the phenomenon of shear bands (*e.g.* [4, 15, 16, 2]) occurring during the high strain-rate deformations of metals. Formation of shear bands is a well known material instability that usually leads to rupture, and has received considerable attention in the mechanics literature (*e.g.* [3, 7, 12, 19, 21]). The reader is referred to [11] for a description of the problem intended for a mathematically oriented reader that is briefly also outlined below.

It was recognized by Zener and Hollomon [22] (see also [13]) that the effect of the deformation speed is twofold: (a) To change the deformation conditions from isothermal to nearly adiabatic; under nearly adiabatic conditions the combined effect of thermal softening and strain hardening tends to produce net softening response. (b) Strain rate has an effect *per se* and induces momentum diffusion that needs to be included in the constitutive modeling. A theory of thermoviscoplasticity is commonly used to model shear bands and we refer to [13, 15, 19, 20, 10] for various accounts of the modeling aspects.

The basic mechanism for localization is encoded in the behavior of the following simple system of differential equations

$$\begin{aligned}
 (2.11) \quad & v_t = \partial_x (\mu(\theta) v_x^n), \\
 & \theta_t = \sigma v_x = \mu(\theta) v_x^{n+1}
 \end{aligned}$$

(which is the adiabatic case $\kappa = 0$ of (2.1)). This model is appropriate for a non-Newtonian fluid with temperature dependent viscosity, and is also a simplification of the models proposed in [22, 13] to capture the mechanism for shear band formation in high strain-rate plastic deformations of metals. The argument - adapted to the language of a temperature dependent fluid - goes as follows: as the fluid gets sheared the dissipation produces heat and elevates the temperature of the fluid. The viscosity decreases with the elevation of the temperature and the fluid becomes softer and easier to shear. One eventuality is that the shear deformation distributes uniformly across the material in the same manner as it does for the usual Newtonian fluids. This arrangement is described by the uniform shearing solution (2.10). A second mode of response is suggested when comparing the behavior of the fluid in two spots: one hot and one cold. Since the viscosity

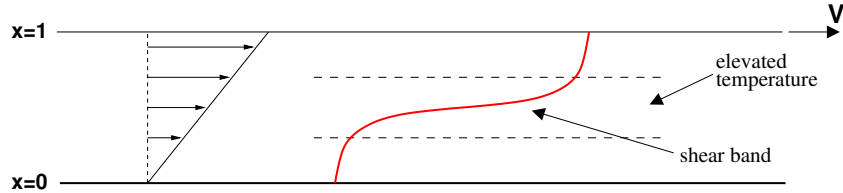


FIGURE 1. Uniform shear versus shear band.

is weaker in the hot spot and stronger in the cold spots, the amount of shear generated in the hot spot will be larger than the shear generated in the cold spot and in turn the temperature difference will be intensified. It is then conceivable that the deformation localizes into a narrow band where the material is considerably hotter (and weaker) than the surrounding environment. The two possibilities are depicted in Fig. 1. The outcome of the competition of thermal softening and momentum diffusion is captured by the behavior of solutions to (2.11).

A series of works analyze the system (2.11) mostly for power law viscosities

$$(H_{pl}) \quad \mu(\theta) = \theta^{-\alpha}, \quad \alpha > 0 \quad \text{and hence} \quad \sigma = \theta^{-\alpha} v_x^n.$$

These studies show stable response [4, 15] when $-\alpha + n > 0$, and indicate unstable response [15, 2, 17] but without characterizing the behavior in the complementary region $-\alpha + n < 0$. More precisely, in the unstable regime Tzavaras [15] shows that development of shear bands can be induced by stress boundary conditions leading to finite-time blow-up, and that their occurrence is associated with a collapse of stress diffusion across the band. On the other hand, Bertsch, Peletier and Verduyn-Lunel [2] show that if the problem has global solutions and there is a sufficiently large initial temperature perturbation, then a shear band appears as the asymptotic in time state. Careful and detailed numerical investigations [19, 6, 1] indicate that instability is widespread in the parameter regime $-\alpha + n < 0$ and is typically followed by the development of shear bands.

The behavior in the “instability domain” is at present poorly understood, especially regarding the precise mechanism of formation of the shear band. The reason is the response in this regime results from the competition between an ill-posed problem and a parabolic regularization, and little mathematical theory is available to study such effects. Nevertheless, an asymptotic theory similar to the Chapman-Enskog expansion is used by Katsaounis-Tzavaras [10, 11] to calculate an effective equation for the compound effect of thermal softening and strain-rate sensitivity. The effective equation changes type from forward to backward parabolic across the instability threshold, and thus provides an asymptotic criterion for the onset of localization. In the present work, we will develop a mathematical framework for studying the competition and for examining the conjecture of [10]. Our analysis is facilitated by the use of the exponential law (H_{exp}) inducing special scaling properties on the resulting system of partial differential equations.

2.3. Hadamard instability. In the mechanics literature shear localization is typically associated with Hadamard-instability. This is easily put on display for (2.1), by considering the limiting case $n = 0$ and $\kappa = 0$. In the parlance of mechanics, this corresponds to rate-insensitive deformations and absence of heat conduction, and leads to the system of conservation laws

$$(2.12) \quad \partial_t \begin{pmatrix} v \\ \theta \end{pmatrix} = \begin{pmatrix} (\mu(\theta))_x \\ \mu(\theta)v_x \end{pmatrix} = \begin{pmatrix} 0 & \mu'(\theta) \\ \mu(\theta) & 0 \end{pmatrix} \partial_x \begin{pmatrix} v \\ \theta \end{pmatrix}$$

For $\mu'(\theta) < 0$ the wave speeds are both imaginary, $\lambda_{\pm} = \pm i\sqrt{|\mu'|\mu}$, and the linearized initial value problem for (2.12) is ill-posed.

Two questions then emerge:

- (i) To assess the combined effect of the competition between Hadamard instability and momentum diffusion and/or heat conduction (as manifested by small $n > 0$ and $\kappa > 0$ respectively).
- (ii) While Hadamard instability indicates the catastrophic growth of oscillations around a mean state, it does not by itself explain the formation of coherent structures typically observed in localization. The latter is an outcome of the nonlinear effects and has to be assessed at the level of the nonlinear problem.

2.4. Formulation via relative perturbations. The first objective is to develop quantitative criteria for the stability of the uniform shearing solutions. Since the basic solutions are time dependent an issue arises how to define their stability. Following [12, 17], we call the uniform shearing solution *asymptotically stable* if perturbations of the solution decay faster than the basic solution, and we call it *unstable* if they grow faster than the uniform shearing solution.

It is expedient to introduce a relative perturbation formulation of the problem: For the *exponential law* (H_{exp}), we introduce the state (U, Θ, Σ) describing the relative perturbation and defined through the transformation

$$\begin{aligned}
 (2.13) \quad u(x, t) &= U(x, t) \\
 \theta(x, t) &= \theta_s(t) + \Theta(x, t) \\
 \sigma(x, t) &= \sigma_s(t) \Sigma(x, t)
 \end{aligned}$$

where (θ_s, σ_s) is given by (2.10) and satisfies in particular that

$$(2.14) \quad \dot{\theta}_s = \sigma_s = e^{-\alpha\theta_s}.$$

Using (2.1) and (2.14) we derive the system satisfied by the relative perturbation (U, Θ, Σ) in the form

$$\begin{aligned}
 (2.15) \quad U_t &= \sigma_s(t) \Sigma_{xx} \\
 \Theta_t - \kappa \Theta_{xx} &= \sigma_s(t) (\Sigma U - 1) \\
 \Sigma &= e^{-\alpha\Theta} U^n
 \end{aligned}$$

Note that the uniform shearing solution is mapped to the state $U_0 = 1$, $\Theta_0 = 0$ and $\Sigma_0 = 1$, and the latter is an equilibrium for the system (2.15). The problem then becomes to study the stability of the equilibrium $(U_0, \Theta_0, \Sigma_0) = (1, 0, 1)$ for the non-autonomous system (2.15).

3. LINEARIZED ANALYSIS OF THE EXPONENTIAL MODEL

In this section we present an analysis of the linearized system. Since the uniform shearing solution is time-dependent the linearized analysis will seek to classify the precise growth in-time of perturbations.

3.1. The linearized problem. We compute the linearized problem, using the ansatz

$$\begin{aligned}
 (3.1) \quad U &= 1 + \delta \bar{u} + O(\delta^2) \\
 \Theta &= \delta \bar{\theta} + O(\delta^2) \\
 \Sigma &= 1 + \delta \bar{\sigma} + O(\delta^2)
 \end{aligned}$$

where δ a small parameter measuring the size of the perturbation and $\delta \ll 1$. Expansion of the equation (2.15)₃ gives to the leading order of δ

$$1 + \delta \bar{\sigma} = 1 + (-\alpha \bar{\theta} + n \bar{u}) \delta + O(\delta^2)$$

while linearizing the other two equations gives

$$\begin{aligned}\bar{u}_t &= \sigma_s(t) \bar{\sigma}_{xx} + O(\delta^2) \\ \bar{\theta}_t - \kappa \bar{\theta}_{xx} &= \sigma_s(t) (\bar{\sigma} + \bar{u}) + O(\delta^2).\end{aligned}$$

Collecting the equations together and neglecting the terms of $O(\delta^2)$ we obtain the linearized system:

$$(3.2) \quad \begin{cases} \bar{u}_t = \sigma_s(t) (n\bar{u}_{xx} - \alpha\bar{\theta}_{xx}) \\ \bar{\theta}_t - \kappa\bar{\theta}_{xx} = \sigma_s(t) ((n+1)\bar{u} - \alpha\bar{\theta}) \\ \bar{\sigma} = n\bar{u} - \alpha\bar{\theta} \end{cases}$$

The boundary conditions (2.4) and (2.5) and the transformations (2.13) and (3.1), imply that the induced boundary conditions for the linearized system are

$$(3.3) \quad \begin{cases} \bar{u}_x(0, t) = \bar{u}_x(1, t) = 0, \\ \bar{\theta}_x(0, t) = \bar{\theta}_x(1, t) = 0. \end{cases}$$

In view of the transformations (2.15) and (3.1), the relation between the original solution (u, σ, θ) and the solution of the linear problem (3.2) is as follows

$$(3.4) \quad \begin{aligned} u &= v_x = 1 + \delta\bar{u}(x, t) + O(\delta^2) \\ \theta &= \frac{1}{\alpha} \log(\alpha t + c_0) + \delta\bar{\theta}(x, t) + O(\delta^2) \\ \sigma &= \frac{1}{\alpha t + c_0} (1 + \delta\bar{\sigma}(x, t) + O(\delta^2)) \end{aligned}$$

3.2. A change of time scale. Our analysis of the linearized equation is facilitated by introducing the transformation of variables

$$(3.5) \quad \begin{aligned} \bar{u}(x, t) &= \hat{u}(x, \tau(t)) \\ \bar{\theta}(x, t) &= \hat{\theta}(x, \tau(t)) \\ \bar{\sigma}(x, t) &= \hat{\sigma}(x, \tau(t)) \end{aligned}$$

where $\tau(t)$ is a rescaling of time, defined by

$$\begin{cases} \frac{d\tau}{dt} = \sigma_s(t) = \frac{1}{\alpha t + c_0} \\ \tau(0) = 0 \end{cases} \implies \tau(t) = \frac{1}{\alpha} \log \left(\frac{c_0 + \alpha t}{c_0} \right).$$

The map $\tau(t)$ is invertible and its inverse is given by

$$t = \hat{t}(\tau) = \frac{c_0}{\alpha} (e^{\alpha\tau} - 1).$$

One computes that $(\hat{u}(x, \tau), \hat{\theta}(x, \tau), \hat{\sigma}(x, \tau))$ satisfy the linear system

$$(3.6) \quad \begin{cases} \frac{\partial \hat{u}}{\partial \tau} = (n\hat{u}_{xx} - \alpha\hat{\theta}_{xx}) \\ \frac{\partial \hat{\theta}}{\partial \tau} - \kappa c_0 e^{\alpha\tau} \hat{\theta}_{xx} = (n+1)\hat{u} - \alpha\hat{\theta} \\ \hat{\sigma} = n\hat{u} - \alpha\hat{\theta} \end{cases}$$

with boundary conditions

$$(3.7) \quad \begin{cases} \hat{u}_x(0, \tau) = \hat{u}_x(1, \tau) = 0, \\ \hat{\theta}_x(0, \tau) = \hat{\theta}_x(1, \tau) = 0. \end{cases}$$

For further reference, we record that the original variables (u, σ, θ) and the solution $(\hat{u}, \hat{\sigma}, \hat{\theta})$ of the rescaled problem (3.6)-(3.7) are related through the formulas

$$(3.8) \quad \begin{aligned} u &= v_x = 1 + \delta \hat{u}(x, \tau(t)) + O(\delta^2) \\ \theta &= \frac{1}{\alpha} \log(\alpha t + c_0) + \delta \hat{\theta}(x, \tau(t)) + O(\delta^2) \\ \sigma &= \frac{1}{\alpha t + c_0} (1 + \delta \hat{\sigma}(x, \tau(t)) + O(\delta^2)) \end{aligned}$$

3.3. Linearized analysis with frozen coefficients. We next consider the system

$$(3.9) \quad \begin{cases} \frac{\partial \hat{u}}{\partial \tau} = (n \hat{u}_{xx} - \alpha \hat{\theta}_{xx}) \\ \frac{\partial \hat{\theta}}{\partial \tau} - k \hat{\theta}_{xx} = (n+1) \hat{u} - \alpha \hat{\theta} \end{cases}$$

with boundary conditions (3.7). Note that in (3.6) the thermal diffusion coefficient $k = k(\tau) = \kappa c_0 e^{\alpha \tau}$ is time dependent, while in (3.9) this coefficient is frozen in time. We analyze the solutions of (3.9) via an eigenvalue analysis. This provides the following information:

- (a) For $k = 0$ it provides the stability or instability properties of the linearized system (3.6).
- (b) For $k > 0$ the eigenvalue analysis will only offer an indication of the effect of thermal diffusion on the linearized analysis. This will be complemented by an energy estimate analysis of the exact system (3.2) in the following section.

The solutions of (3.9)-(3.7) are expressed as a cosine Fourier series

$$(3.10) \quad \begin{aligned} \hat{u}(x, \tau) &= \sum_{j=0}^{\infty} \hat{u}_j(\tau) \cos j\pi x \\ \hat{\theta}(x, t) &= \sum_{j=0}^{\infty} \hat{\theta}_j(\tau) \cos j\pi x \end{aligned}$$

where the Fourier coefficients $(\hat{u}_j(\tau), \hat{\theta}_j(\tau))$ satisfy the ordinary differential equations

$$(3.11) \quad \begin{aligned} \frac{d}{dt} \begin{pmatrix} \hat{u}_j \\ \hat{\theta}_j \end{pmatrix} &= \begin{pmatrix} 0 & 0 \\ 0 & -k(j\pi)^2 \end{pmatrix} \begin{pmatrix} \hat{u}_j \\ \hat{\theta}_j \end{pmatrix} + \begin{pmatrix} -n(j\pi)^2 & \alpha(j\pi)^2 \\ n+1 & -\alpha \end{pmatrix} \begin{pmatrix} \hat{u}_j \\ \hat{\theta}_j \end{pmatrix} \\ &= \begin{pmatrix} -n(j\pi)^2 & \alpha(j\pi)^2 \\ n+1 & -\alpha - k(j\pi)^2 \end{pmatrix} \begin{pmatrix} \hat{u}_j \\ \hat{\theta}_j \end{pmatrix} \end{aligned}$$

The eigenvalues of the matrix

$$A := \begin{pmatrix} -n(j\pi)^2 & \alpha(j\pi)^2 \\ n+1 & -\alpha - k(j\pi)^2 \end{pmatrix}$$

are the roots of the binomial equation

$$(3.12) \quad \lambda^2 + \lambda(\alpha + n(j\pi)^2 + k(j\pi)^2) + nk(j\pi)^4 - \alpha(j\pi)^2 = 0, \quad j = 0, 1, 2, \dots$$

The mode $j = 0$. For $j = 0$ the equation becomes $\lambda^2 + \alpha\lambda = 0$ and has two eigenvalues $\lambda_{0,0} = 0$ and $\lambda_{-,0} = -\alpha$. This corresponds to marginal stability for the linearized system. A closer look

shows that the system (3.11) for $j = 0$ takes the form

$$\begin{aligned}\frac{d\hat{u}_0}{d\tau} &= 0 \\ \frac{d\hat{\theta}_0}{d\tau} &= (n+1)\hat{u}_0 - \alpha\hat{\theta}_0\end{aligned}$$

This implies, using (3.10), (3.4), (2.2) and the boundary condition (2.3), that

$$\hat{u}_0(\tau) = \hat{u}_0(0) = \int_0^1 \bar{u}(x, 0) dx = 0.$$

and clearly $\hat{\theta}_0(\tau)$ decays. Thus, the 0-th mode decays.

The modes $j = 1, 2, \dots$ For these modes the eigenvalues are

$$(3.13) \quad \lambda_{\pm, j} = -\frac{1}{2}(\alpha + n(j\pi)^2 + k(j\pi)^2) \pm \frac{1}{2}\sqrt{\Delta_j}$$

where the discriminant

$$\begin{aligned}\Delta_j &:= ((n+k)(j\pi)^2 + \alpha)^2 + 4\alpha(j\pi)^2 - 4nk(j\pi)^4 \\ &= (n-k)^2(j\pi)^4 + (2\alpha(n+k) + 4\alpha)(j\pi)^2 + \alpha^2 > 0\end{aligned}$$

Since

$$\lambda_{j,+} + \lambda_{j,-} = -(n+k)(j\pi)^2 - \alpha < 0, \quad \lambda_{j,+}\lambda_{j,-} = nk(j\pi)^4 - \alpha(j\pi)^2$$

we conclude that

$$(3.14) \quad \begin{aligned} \text{the } j\text{-th mode is asymptotically stable} & \quad \text{iff} \quad nk(j\pi)^2 > \alpha \\ \text{the } j\text{-th mode is unstable} & \quad \text{iff} \quad nk(j\pi)^2 < \alpha \end{aligned}$$

In summary:

- (i) If $k = 0$ then all modes $j = 1, 2, \dots$ are unstable.
- (ii) If $k > 0$ the first few modes might be unstable, that is the modes j for which $nk(j\pi)^2 < \alpha$, but the high frequency modes are stable.
- (iii) The higher k the fewer the number of unstable modes. For k larger than a certain threshold (here equal to $\alpha/(n\pi^2)$) all modes are asymptotically stable.

3.4. Asymptotics of the modes and the nature of the instability. We analyze the behavior of the linearized modes as a function of j and discuss the nature of the instability in the various special cases of interest. The analysis reveals the role of the parameters n, k regarding the nature of the instability

3.4.1. Case 1: $k = 0, n = 0$, Hadamard instability. In this regime

$$\lambda_{\pm, j} = -\frac{\alpha}{2} \pm \frac{1}{2}\sqrt{\alpha^2 + 4\alpha(j\pi)^2}$$

one eigenvalue is negative and the other strictly positive and increasing with j . Using the Taylor series development

$$(3.15) \quad \sqrt{1+x} = 1 + \frac{1}{2}x - \frac{1}{4}x^2 + \frac{3}{8}x^3 + \dots, \quad \text{for } 0 < x \ll 1$$

we obtain the following asymptotic developments for the eigenvalues

$$(3.16) \quad \begin{aligned} \lambda_{-, j} &= -\sqrt{\alpha}j\pi - \frac{\alpha}{2} - \frac{1}{8}\frac{\alpha^{\frac{3}{2}}}{j\pi} + O\left(\frac{1}{j^3}\right) \\ \lambda_{+, j} &= \sqrt{\alpha}j\pi - \frac{\alpha}{2} + \frac{1}{8}\frac{\alpha^{\frac{3}{2}}}{j\pi} + O\left(\frac{1}{j^3}\right). \end{aligned}$$

Referring to the formulas (3.8), (3.5) and (3.16), we see that the j -th mode of the perturbation grows to the leading order like

$$\begin{aligned}\bar{\theta}_j(x, t) &= \cos(j\pi x) e^{\lambda_{+,j}\tau(t)} \sim \cos(j\pi x) \exp \left\{ \sqrt{\alpha} j\pi \frac{1}{\alpha} \log \left(\frac{c_0 + \alpha t}{c_0} \right) \right\} \\ &= \cos(j\pi x) \left(\frac{c_0 + \alpha t}{c_0} \right)^{\frac{j\pi}{\sqrt{\alpha}}}\end{aligned}$$

Clearly the perturbation grows much faster than the uniform shearing solution $\theta_s(t)$ given by (2.10) where the growth is logarithmic, and the behavior is characteristic of *Hadamard instability*, that is the high frequency oscillations grow at a catastrophic rate.

3.4.2. *Case 2: $k = 0$, $n > 0$, Turing instability.* In this case the eigenvalues of the j -th mode are given by the formulas

$$\lambda_{\pm,j} = -\frac{\alpha + n(j\pi)^2}{2} \pm \frac{1}{2}(\alpha + n(j\pi)^2) \sqrt{1 + \frac{4\alpha(j\pi)^2}{(\alpha + n(j\pi)^2)^2}}$$

Again we have one negative and one positive eigenvalue and thus unstable response in this regime as well. Using once again the Taylor expansion (3.15) we obtain the asymptotic expansions

$$\begin{aligned}(3.17) \quad \lambda_{-,j} &= -n(j\pi)^2 - \alpha - \frac{\alpha(j\pi)^2}{\alpha + n(j\pi)^2} + O\left(\frac{1}{j^2}\right) \\ \lambda_{+,j} &= \frac{\alpha(j\pi)^2}{\alpha + n(j\pi)^2} + O\left(\frac{1}{j^2}\right).\end{aligned}$$

for the positive and negative eigenvalues respectively.

Lemma 3.1. *The positive eigenvalue $\lambda_{+,j}$ satisfies the following properties:*

$$\begin{aligned}(3.18) \quad &\lambda_{+,j} \text{ is increasing in } j \\ (3.19) \quad &\lambda_{+,j} < \frac{\alpha}{n} \\ (3.20) \quad &\lambda_{+,j} \rightarrow \frac{\alpha}{n} \quad \text{as } j \rightarrow \infty\end{aligned}$$

Proof. Set $x = (j\pi)^2$ and recall that

$$\lambda_+(x) = -\frac{\alpha + nx}{2} + \frac{1}{2}\sqrt{(nx + \alpha)^2 + 4\alpha x}$$

satisfies the identity

$$(3.21) \quad \lambda_+^2(x) + \lambda_+(x)(nx + \alpha) - \alpha x = 0.$$

Differentiating (3.21), we derive

$$\frac{\partial \lambda_+}{\partial x}(x) = \frac{\alpha - \lambda_+(x)n}{2\lambda_+(x) + (nx + \alpha)} = \frac{\alpha - \lambda_+(x)n}{\sqrt{(nx + \alpha)^2 + 4\alpha x}}.$$

Next, using the elementary bound $\sqrt{1+z} < 1 + \frac{1}{2}z$ for $z > 0$ we obtain

$$\begin{aligned}\lambda_+(x) &= -\frac{\alpha + nx}{2} + \frac{1}{2}(nx + \alpha) \sqrt{1 + \frac{4\alpha x}{(nx + \alpha)^2}} \\ &< \frac{\alpha x}{nx + \alpha} < \frac{\alpha}{n}\end{aligned}$$

This shows that $\frac{\partial \lambda_+}{\partial x}(x) > 0$ and provides (3.18) and (3.19). Then (3.20) follows from (3.17). \square

The following remarks are in order: Observe first that, by virtue of (3.8), (3.5) and (3.16), the j -th mode of the perturbation grows like

$$(3.22) \quad \begin{aligned} \bar{\theta}_j(x, t) &= \cos(j\pi x) e^{\lambda_{+,j}\tau(t)} = \cos(j\pi x) \exp \left\{ \left(\frac{\alpha(j\pi)^2}{\alpha + n(j\pi)^2} + O\left(\frac{1}{j^2}\right) \right) \frac{1}{\alpha} \log \left(\frac{c_0 + \alpha t}{c_0} \right) \right\} \\ &\sim \cos(j\pi x) \left(\frac{c_0 + \alpha t}{c_0} \right)^{\frac{1}{n}} \end{aligned}$$

Clearly the perturbation grows much faster than the uniform shearing solution $\theta_s(t)$, but the rate of growth is bounded in j . On the other hand, the growth becomes very fast as the rate sensitivity $n \rightarrow 0$.

The behavior in this regime is characterized by *Turing instability*. Recall, that Turing instability [14] corresponds to the following scenario that occurs in some instances of dynamical systems. There are two dynamical systems

$$\dot{x} = Ax, \quad \dot{x} = Bx$$

where the spectrum of both matrices A and B lies in the left-hand plane, but the Trotter product of the two systems

$$\dot{x} = (A + B)x$$

exhibits unstable response.

Indeed, the dynamical system (3.11) with $k = 0$ may be visualized as the Trotter product of the two systems

$$(3.23) \quad \frac{d}{dt} \begin{pmatrix} \hat{u}_j \\ \hat{\theta}_j \end{pmatrix} = \begin{pmatrix} -\frac{1}{2}n(j\pi)^2 & \alpha(j\pi)^2 \\ 0 & -\frac{1}{2}\alpha \end{pmatrix} \begin{pmatrix} \hat{u}_j \\ \hat{\theta}_j \end{pmatrix}$$

and

$$(3.24) \quad \frac{d}{dt} \begin{pmatrix} \hat{u}_j \\ \hat{\theta}_j \end{pmatrix} = \begin{pmatrix} -\frac{1}{2}n(j\pi)^2 & 0 \\ n+1 & -\frac{1}{2}\alpha \end{pmatrix} \begin{pmatrix} \hat{u}_j \\ \hat{\theta}_j \end{pmatrix}$$

Each of (3.23) and (3.24) has spectrum in the left half space but the eigenvalues of (3.11) have unstable response.

3.4.3. Case 3: $k > 0$, $n > 0$, thermal diffusion stabilizes the high modes. In this regime the eigenvalues are given by (3.13) and they are real and have the properties

$$(3.25) \quad \lambda_{-,j} < 0 \quad \forall j$$

$$(3.26) \quad \lambda_{+,j} < 0 \quad \Longleftrightarrow \quad k(j\pi)^2 > \frac{\alpha}{n}$$

Therefore, the high modes are stable, but the low modes might be unstable if k is sufficiently small. The “most unstable” mode is the first mode.

One can again carry out the large j asymptotics of the eigenvalues. The result, in the case that $n > k$, reads

$$(3.27) \quad \begin{aligned} \lambda_{-,j} &= -n(j\pi)^2 - \alpha - \frac{\alpha(k+1)}{\left|n - k + \frac{\alpha}{(j\pi)^2}\right|} + O\left(\frac{1}{j^2}\right), \\ \lambda_{+,j} &= -k(j\pi)^2 + \frac{\alpha(k+1)}{\left|n - k + \frac{\alpha}{(j\pi)^2}\right|} + O\left(\frac{1}{j^2}\right). \end{aligned}$$

A similar formula holds when $n < k$.

3.5. Effect of thermal diffusion on the linearized problem. Consider now the linearized system (3.2) with boundary condition (3.3). Since we are interested in perturbations of the uniform shearing solution we will consider initial data that satisfy $\int_0^1 u_0 dx = 0$ and thus focus on solutions with

$$(3.28) \quad \int_0^1 u(x, t) dx = 0$$

The objective is now to analyze the effect of the time-dependent diffusion on the dynamics of the system. The linearized analysis of the system with frozen coefficients suggests to expect that diffusion stabilizes the system and its effect is intensified with the passage of time. Indeed, here we provide a rigorous proof of this statement via energy estimates.

Lemma 3.2. *There exist $A > 0$ and $T > 0$ such that*

$$(3.29) \quad \int_0^1 \left(\frac{A}{2} \bar{u}^2 + \frac{1}{2} \bar{\theta}^2 \right) (x, t) dx \leq \int_0^1 \left(\frac{A}{2} \bar{u}^2 + \frac{1}{2} \bar{\theta}^2 \right) (x, T) dx \quad \text{for } t \geq T$$

and

$$(3.30) \quad \int_0^1 \left(\frac{A}{2} \bar{u}^2 + \frac{1}{2} \bar{\theta}^2 \right) (x, t) dx \rightarrow 0 \quad \text{as } t \rightarrow \infty.$$

Proof. We multiply (3.2)₁ by \bar{u} and (3.2)₂ by $\bar{\theta}$ and obtain the identities

$$\begin{aligned} \frac{d}{dt} \int_0^1 \frac{1}{2} \bar{u}^2 dx + n \sigma_s(t) \int_0^1 \bar{u}_x^2 dx &= \alpha \sigma_s(t) \int_0^1 \bar{\theta}_x \bar{u}_x dx \\ \frac{d}{dt} \int_0^1 \frac{1}{2} \bar{\theta}^2 dx + \kappa \int_0^1 \bar{\theta}_x^2 dx + \alpha \sigma_s(t) \int_0^1 \bar{\theta}^2 dx &= (n+1) \sigma_s(t) \int_0^1 \bar{u} \bar{\theta} dx \end{aligned}$$

Using Cauchy-Schwarz inequality, gives

$$(3.31) \quad \begin{aligned} \frac{d}{dt} \int_0^1 \frac{1}{2} \bar{u}^2 dx + \frac{n}{2} \sigma_s(t) \int_0^1 \bar{u}_x^2 dx &\leq \frac{\alpha^2}{2n} \sigma_s(t) \int_0^1 \bar{\theta}_x^2 dx \\ \frac{d}{dt} \int_0^1 \frac{1}{2} \bar{\theta}^2 dx + \kappa \int_0^1 \bar{\theta}_x^2 dx + \frac{\alpha}{2} \sigma_s(t) \int_0^1 \bar{\theta}^2 dx &\leq \frac{(n+1)^2}{2\alpha} \sigma_s(t) \int_0^1 \bar{u}^2 dx. \end{aligned}$$

In view of (3.28), we may use the Poincare inequality

$$(3.32) \quad \int_0^1 \bar{u}^2 dx \leq C_p \int_0^1 \bar{u}_x^2 dx.$$

Combining the above, we note that for A a positive constant we have

$$\begin{aligned} \frac{d}{dt} \int_0^1 \left(\frac{A}{2} \bar{u}^2 + \frac{1}{2} \bar{\theta}^2 \right) dx + \frac{An}{2C_p} \sigma_s(t) \int_0^1 \bar{u}_x^2 dx + \frac{\alpha}{2} \sigma_s(t) \int_0^1 \bar{\theta}^2 dx + \kappa \int_0^1 \bar{\theta}_x^2 dx \\ \leq \frac{A\alpha^2}{2n} \sigma_s(t) \int_0^1 \bar{\theta}_x^2 dx + \frac{(n+1)^2}{2\alpha} \sigma_s(t) \int_0^1 \bar{u}^2 dx. \end{aligned}$$

Next we select A such that $\frac{An}{2C_p} \geq \frac{(n+1)^2}{\alpha}$, and deduce that for A thus selected there is a choice $c = c(A) > 0$ such that

$$\begin{aligned} \frac{d}{dt} \int_0^1 \left(\frac{A}{2} \bar{u}^2 + \frac{1}{2} \bar{\theta}^2 \right) dx + c \sigma_s(t) \int_0^1 \left(\frac{A}{2} \bar{u}^2 + \frac{1}{2} \bar{\theta}^2 \right) dx + \kappa \int_0^1 \bar{\theta}_x^2 dx \\ \leq \frac{A\alpha^2}{2n} \sigma_s(t) \int_0^1 \bar{\theta}_x^2 dx. \end{aligned}$$

Select now T such that $\frac{A\alpha^2}{2n}\sigma_s(t) < \kappa$ for $t \geq T$ (recall from (1.2) that $\sigma_s(t) \rightarrow 0$ when $t \rightarrow \infty$). On the interval $t \geq T$, we have the differential inequality

$$\frac{d}{dt} \int_0^1 \left(\frac{A}{2} \bar{u}^2 + \frac{1}{2} \bar{\theta}^2 \right) dx + c\sigma_s(t) \int_0^1 \left(\frac{A}{2} \bar{u}^2 + \frac{1}{2} \bar{\theta}^2 \right) dx \leq 0.$$

The latter implies (3.29) and yields, upon using Gronwall's inequality and (2.10),

$$\int_0^1 \left(\frac{A}{2} \bar{u}^2 + \frac{1}{2} \bar{\theta}^2 \right) (x, t) dx \leq \left(\int_0^1 \left(\frac{A}{2} \bar{u}^2 + \frac{1}{2} \bar{\theta}^2 \right) (x, T) dx \right) \exp \left\{ -c \int_T^t \sigma_s(z) dz \right\} \rightarrow 0, \quad \text{as } t \rightarrow \infty,$$

and concludes the proof \square

The next lemma provides control of the intermediate times.

Lemma 3.3. *There exist $B > 0$ and a constant $C_B > 0$ such that*

$$(3.33) \quad \int_0^1 \left(\frac{1}{2} \bar{u}^2 + \frac{B}{2} \bar{\theta}^2 \right) (x, t) dx \leq \left(\int_0^1 \left(\frac{1}{2} \bar{u}^2 + \frac{B}{2} \bar{\theta}^2 \right) (x, 0) dx \right) \exp\{C_B t\} \quad \text{for } t \geq 0.$$

Proof. Using again (3.31) and (3.32) we have for any $B > 0$

$$\begin{aligned} \frac{d}{dt} \int_0^1 \left(\frac{1}{2} \bar{u}^2 + \frac{B}{2} \bar{\theta}^2 \right) dx + \frac{n}{2C_p} \sigma_s(t) \int_0^1 \bar{u}^2 dx + \frac{B\alpha}{2} \sigma_s(t) \int_0^1 \bar{\theta}^2 dx + B\kappa \int_0^1 \bar{\theta}_x^2 dx \\ \leq \frac{\alpha^2}{2n} \sigma_s(t) \int_0^1 \bar{\theta}_x^2 dx + B \frac{(n+1)^2}{2\alpha} \sigma_s(t) \int_0^1 \bar{u}^2 dx \end{aligned}$$

Select now B large so that $B\kappa > \frac{\alpha^2}{2n} \sigma_s(t)$ for all $t \geq 0$, and then we obtain

$$\frac{d}{dt} \int_0^1 \left(\frac{1}{2} \bar{u}^2 + \frac{B}{2} \bar{\theta}^2 \right) dx \leq C_B \int_0^1 \left(\frac{1}{2} \bar{u}^2 + \frac{B}{2} \bar{\theta}^2 \right) dx$$

from where (3.33) follows via Gronwall's inequality. \square

We conclude now the analysis of stability. Suppose that for some $\delta > 0$ the initial data satisfy $\int_0^1 u_0 = 0$ and are controlled in L^2 by

$$\int_0^1 \left(\frac{1}{2} \bar{u}^2 + \frac{B}{2} \bar{\theta}^2 \right) (x, 0) dx \leq \delta$$

Then (3.29), (3.33) imply

$$(3.34) \quad \begin{aligned} \int_0^1 \left(\frac{1}{2} \bar{u}^2 + \frac{B}{2} \bar{\theta}^2 \right) (x, t) dx &\leq \delta e^{C_B t} \quad \text{for } t \geq 0 \\ \int_0^1 \left(\frac{A}{2} \bar{u}^2 + \frac{1}{2} \bar{\theta}^2 \right) (x, t) dx &\leq A \delta e^{C_B T} \quad \text{for } t \geq T \end{aligned}$$

Together they imply that the state $(0, 0)$ is stable in L^2 , and in fact on account of (3.30) it is asymptotically stable. We state the result in the following:

Proposition 3.4. *For the initial-boundary value problem (3.2), (3.3) with $\kappa > 0$, if the initial perturbation $(\bar{u}_0, \bar{\theta}_0)$ satisfies $\int_0^1 \bar{u}_0 dx = 0$ then the equilibrium $(0, 0)$ is asymptotically stable in L^2 .*

The proof of the above lemmas and the analysis of the linearized problem with frozen coefficients indicate that the perturbation of the base solution may drift far from the origin until eventually it is recaptured as the effect of the diffusion intensifies with time.

This phenomenon of *metastability* also appears in numerical runs for the nonlinear problem; an instance of these runs appears in Figure 2. We solve numerically the rescaled system (4.2) for

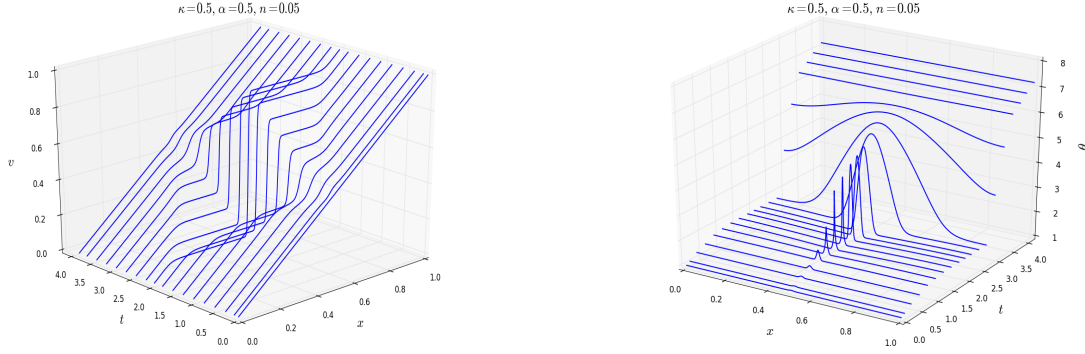


FIGURE 2. Metastability for the nonlinear problem : $v(x,t)$ (left), $\theta(x,t)$ (right).

$\kappa = 0.5$, $\alpha = 0.5$, $n = 0.05$. The initial conditions are perturbations of the uniform shearing solutions and they are : $v(x,0) = x$ and $\theta(x,0) = 1 + \delta(x)$, where $\delta(x)$ is a small Gaussian perturbation centered at the middle of the interval. The numerical method is based on adaptivity in space and time. An adaptive finite element method is used for the spatial discretisation while a Runge-Kutta method with variable time step is used for the discretisation in time. Further details concerning the numerical scheme and the adaptivity criteria can be found in [1]. In Figure 2 the evolution in time is presented for the original variables v and θ in (4.1). We notice that, after a transient period of localization, thermal diffusion dominates the process, inhomogeneities of the state variables dissipate, and eventually the solution approaches a uniform shearing solution (2.8).

4. LOCALIZATION - PART I

We consider next the problem (2.1) on the whole real line and put aside the boundary conditions. The objective is to construct special solutions that capture a process of localization. This is done over three sections. The present one is preliminary in nature and discusses various properties that make the construction feasible and the setting of the problem. The main step is performed in section 5 where a special class of self-similar solutions are constructed. The localized solutions are then presented in section 6.

4.1. Relative perturbations and a change of time scale. We consider (2.1) on $\mathbb{R} \times (0, \infty)$ and recall the notation $u = v_x$. The uniform shearing solutions (2.8) are defined by solving (2.9). Introduce the transformation

$$\begin{aligned}
 (4.1) \quad u(x,t) &= \hat{U}(x, \tau(t)) \\
 \theta(x,t) &= \theta_s(t) + \hat{\Theta}(x, \tau(t)) \\
 \sigma(x,t) &= \sigma_s(t) \hat{\Sigma}(x, \tau(t))
 \end{aligned}$$

which involves a passage to relative perturbations and a change of time scale from the original to a rescaled time $\tau(t)$. The scaling $\tau(t)$ is defined by

$$\tau(t) = \frac{1}{\alpha} \log \left(\frac{c_0 + \alpha t}{c_0} \right) = \theta_s(t) - \theta_s(0),$$

it satisfies

$$\begin{cases} \frac{d\tau}{dt} = \frac{d\theta_s}{dt} = \sigma_s(t) = e^{-\alpha\theta_s} \\ \tau(0) = 0 \end{cases}$$

where $\theta_s(t)$ is as in (2.10), $c_0 = e^{\alpha\theta_0}$. The scaling $\tau(t)$ satisfies $\tau(t) \rightarrow \infty$ as $t \rightarrow \infty$, and $\tau(t)$ is invertible with inverse map given by

$$t = \hat{t}(\tau) = \frac{c_0}{\alpha} (e^{\alpha\tau} - 1) .$$

The functions $(\hat{U}(x, \tau), \hat{\Theta}(x, \tau), \hat{\Sigma}(x, \tau))$ satisfy the system of partial differential equations

$$\begin{aligned} \hat{U}_\tau &= \hat{\Sigma}_{xx} \\ \hat{\Theta}_\tau - \kappa c_0 e^{\alpha\tau} \hat{\Theta}_{xx} &= (\hat{\Sigma} \hat{U} - 1) \\ \hat{\Sigma} &= e^{-\alpha\hat{\Theta}} \hat{U}^n \end{aligned} \tag{4.2}$$

We emphasize that

- For $\kappa > 0$ the system is non-autonomous, which is natural in view of the nature of the transformation (4.1).
- Notably, for $\kappa = 0$ the system (4.2) becomes autonomous.

4.2. Effective equation for the adiabatic system. Next, we consider the adiabatic case $\kappa = 0$ where (4.2) takes the form

$$\begin{aligned} \hat{U}_\tau &= \hat{\Sigma}_{xx} \\ \hat{\Theta}_\tau &= (\hat{\Sigma} \hat{U} - 1) \\ \hat{\Sigma} &= e^{-\alpha\hat{\Theta}} \hat{U}^n . \end{aligned} \tag{4.3}$$

To understand the long time response of (4.3) we perform a formal asymptotic analysis following ideas from [10]. Fix an observational time scale T and introduce the change of variables

$$\begin{aligned} \hat{U}(x, \tau) &= \tilde{U}_T \left(\frac{x}{\sqrt{T}}, \frac{\tau}{T} \right) \\ \hat{\Sigma}(x, \tau) &= \tilde{\Sigma}_T \left(\frac{x}{\sqrt{T}}, \frac{\tau}{T} \right) \\ \hat{\Theta}(x, \tau) &= \tilde{\Theta}_T \left(\frac{x}{\sqrt{T}}, \frac{\tau}{T} \right) \end{aligned}$$

One easily checks that $(\tilde{U}_T(y, s), \tilde{\Sigma}_T(y, s), \tilde{\Theta}_T(y, s))$ satisfies the system

$$\begin{aligned} \tilde{U}_s &= \tilde{\Sigma}_{yy} \\ \frac{1}{T} \tilde{\Theta}_s &= (\tilde{\Sigma} \tilde{U} - 1) \\ \tilde{\Sigma} &= e^{-\alpha\tilde{\Theta}} \tilde{U}^n \end{aligned} \tag{4.4}$$

We are interested in calculating the equation describing the effective response of (4.4) for T sufficiently large. This asymptotic analysis involves a parabolic equation (4.4)₁, which can be thought as a moment equation, and equations (4.4)₂ and (4.4)₃, which may be thought as describing a relaxation process towards the equilibrium curve described by

$$\begin{aligned} \tilde{\Sigma} \tilde{U} - 1 &= 0 \\ \tilde{\Sigma} &= e^{-\alpha\tilde{\Theta}} \tilde{U}^n \end{aligned} \iff \tilde{\Sigma} = \frac{1}{\tilde{U}}, \quad \tilde{\Theta} = \frac{n+1}{\alpha} \log \tilde{U} .$$

Note that the equilibria are a one-dimensional curve parametrized by \tilde{U} .

To calculate the effective equation we perform a procedure analogous to the Chapman-Enskog expansion of kinetic theory. We refer to [11, Sec 5] for the details of the asymptotic analysis. The procedure produces the following effective equation

$$(4.5) \quad u_s = \partial_{yy} \left(\frac{1}{u} \right) + \frac{1}{T} \frac{n+1}{\alpha} \partial_{yy} \left(\frac{1}{u^2} \partial_{yy} \frac{1}{u} \right),$$

which captures the effective response up to order $O(\frac{1}{T^2})$. The leading term is backward parabolic and the first order correction is fourth order. One checks that the effect of the fourth order term is to stabilize the equation, in the sense that the linearized equation around the equilibrium $u_0 = 1$ is stable (see [11] for the details).

It was further shown in [11] that (4.5) admits special solutions that exhibit localization, which is not surprising as the leading response in (4.5) is backward parabolic. Localized solutions of a similar nature will be constructed here directly for the system (4.3). This is a more “unexpected” behavior, because (4.3) is at least *pro-forma* a “hyperbolic-parabolic” system, and the explanation for this behavior lies precisely in the asymptotic relation between (4.3) and (4.5).

4.3. Invariance properties and a related ansatz. It is easy to check that for $\kappa = 0$ the system (4.2) is invariant under the one-parameter scaling transformation

$$(4.6) \quad \begin{aligned} \hat{U}_a(x, \tau) &= a \hat{U}(ax, \tau) \\ \hat{\Sigma}_a(x, \tau) &= \frac{1}{a} \hat{\Sigma}(ax, \tau) \\ \hat{\Theta}_a(x, \tau) &= \frac{n+1}{\alpha} \log a + \hat{\Theta}(ax, \tau) \end{aligned}$$

for any $a > 0$. It is also easy to check that this is the only scaling transformation under which the problem is invariant. This transformation has the distinctive feature that the scaling of space is independent of the scaling of time. Finally, the system (4.2) is not scaling invariant when the thermal diffusion κ is positive.

The scaling invariance (4.6) motivates a change of variables and a related *ansatz* of solutions. Introduce a variable in time scaling $r(\tau)$, the variable $\xi = \frac{x}{r(\tau)}$, and the change of variables

$$(4.7) \quad \begin{aligned} \hat{U}(x, \tau) &= \frac{1}{r(\tau)} \bar{U}\left(\frac{x}{r(\tau)}, \tau\right) \\ \hat{\Sigma}(x, \tau) &= r(\tau) \bar{\Sigma}\left(\frac{x}{r(\tau)}, \tau\right) \\ \hat{\Theta}(x, \tau) &= -\frac{n+1}{\alpha} \log r(\tau) + \bar{\Theta}\left(\frac{x}{r(\tau)}, \tau\right) \end{aligned}$$

We denote by $\dot{r} = \frac{d}{d\tau} r(\tau)$ and by $' = \frac{d}{d\xi}$. Introducing (4.7) to (4.2), we obtain that the function $(\bar{U}(\xi, \tau), \bar{\Sigma}(\xi, \tau), \bar{\Theta}(\xi, \tau))$ satisfies the system of partial differential equations

$$(4.8) \quad \begin{aligned} \bar{U}_\tau - \frac{\dot{r}}{r} (\xi \bar{U})_\xi &= \bar{\Sigma}_{\xi\xi} \\ \bar{\Theta}_\tau - \frac{\dot{r}}{r} \left(\frac{n+1}{\alpha} + \xi \bar{\Theta}_\xi \right) - \kappa c_0 \frac{e^{\alpha\tau}}{r^2(\tau)} \bar{\Theta}_{\xi\xi} &= (\bar{\Sigma} \bar{U} - 1) \\ \bar{\Sigma} &= e^{-\alpha \bar{\Theta}} \bar{U}^n \end{aligned}$$

The resulting system (4.8) depends on the choice of the scaling function $r(\tau)$. We will be interested in solutions that are steady states in the new variables. Of course such solutions are

dynamically evolving in the original variables. There are two case that produce simplified results of interest:

- (a) Consider the case $\kappa > 0$, and select $r(\tau) = e^{\frac{1}{2}\alpha\tau}$. Then the system (4.8) is consistent with the ansatz of steady state solutions $(\bar{U}(\xi), \bar{\Sigma}(\xi), \bar{\Theta}(\xi))$ and the latter are constructed by solving the system of ordinary differential equations

$$(4.9) \quad \begin{aligned} -\frac{\alpha}{2}(\xi\bar{U})' &= \bar{\Sigma}'' \\ -\frac{\alpha}{2}\left(\frac{n+1}{\alpha} + \xi\bar{\Theta}'\right) - \kappa c_0\bar{\Theta}'' &= \bar{\Sigma}\bar{U} - 1 \\ \bar{\Sigma} &= e^{-\alpha\bar{\Theta}}\bar{U}^n \end{aligned}$$

Since $r(\tau) \rightarrow \infty$ as τ increases, solutions of (4.9) will produce defocusing solutions for (4.8). A study of (4.9) is expected to give information about the convergence to the uniform shearing state in the non adiabatic setting. This is not the focus of the present work and we will not deal further with the system (4.9).

- (b) Instead we consider the case $\kappa = 0$. We may now select any exponential function for $r(\tau)$ but are most interested in $r(\tau) = e^{-\lambda\tau}$ with $\lambda > 0$ as this produces focusing solutions. With this selection, $(\bar{U}(\xi), \bar{\Sigma}(\xi), \bar{\Theta}(\xi))$ is a steady solution for (4.8) with $\kappa = 0$ provided it satisfies

$$(4.10) \quad \begin{aligned} \bar{\Sigma}'' &= \lambda(\xi\bar{U})' \\ \lambda\left(\frac{n+1}{\alpha} + \xi\bar{\Theta}'\right) &= \bar{\Sigma}\bar{U} - 1 \\ \bar{\Sigma} &= e^{-\alpha\bar{\Theta}}\bar{U}^n \end{aligned}$$

where $\lambda > 0$ is a parameter.

Remark 4.1. Note that:

- The form of the transformation (4.7) is motivated by the scaling invariance (4.6).
- The scaling connects the two variables and produces interesting systems even in the case κ positive when the system (4.2) is not scale invariant.

5. THE AUXILIARY PROBLEM

In this section we consider the system of ordinary differential equations

$$(5.1) \quad \begin{aligned} \Sigma' &= \xi U \\ \nu\left(\frac{n+1}{\alpha} + \xi\Theta'\right) &= \Sigma U - 1 \\ \Sigma &= e^{-\alpha\Theta}U^n, \end{aligned}$$

on the domain $0 < \xi < \infty$ with $\nu > 0$, subject to the initial condition

$$(5.2) \quad \Sigma(0) = \Sigma_0 > 0.$$

This is an auxiliary problem that will be studied in detail in this section. We emphasize that it does not coincide with the integrated form of (4.10), however it will be used together with additional properties in order to construct solutions of (4.10) and localizing solutions for (4.3) in the following section.

In this section, we are interested in constructing solutions $(U(\xi), \Sigma(\xi), \Theta(\xi))$ for the singular initial value problem (5.1), (5.2) for any $\nu > 0$. The following elementary remarks are in order:

(a) When $\nu = 0$, (5.1) simplifies to

$$(5.3) \quad \begin{cases} \Sigma' = \xi U \\ \Sigma(0) = \Sigma_0 \end{cases} \quad \begin{cases} \Sigma U = 1 \\ \Theta = \frac{n+1}{\alpha} \log U \end{cases}$$

The solution of (5.3) is computed explicitly by

$$(5.4) \quad \begin{aligned} \Sigma(\xi) &= \sqrt{\xi^2 + \Sigma_0^2} \\ U(\xi) &= \frac{1}{\Sigma(\xi)} = \frac{1}{\sqrt{\xi^2 + \Sigma_0^2}} \\ \Theta(\xi) &= -\frac{n+1}{\alpha} \log \sqrt{\xi^2 + \Sigma_0^2}. \end{aligned}$$

(b) When $\nu > 0$, the system (5.1) is invariant under the family of scaling transformations

$$(5.5) \quad \begin{aligned} U_b(\xi) &= bU(b\xi) \\ \Sigma_b(\xi) &= \frac{1}{b}\Sigma(b\xi) \\ \Theta_b(\xi) &= \frac{n+1}{\alpha} \log b + \Theta(b\xi) \end{aligned}$$

for $b > 0$. There is a special solution of (5.1) that is self-similar with respect to the scaling invariance (5.5) and reads

$$(5.6) \quad \hat{\Sigma}(\xi) = \xi, \quad \hat{U}(\xi) = \frac{1}{\xi}, \quad \hat{\Theta}(\xi) = -\frac{n+1}{\alpha} \log \xi.$$

This solution does not however satisfy the initial condition (5.2).

We next construct a function $(U(\xi), \Sigma(\xi), \Theta(\xi))$ which satisfies (5.1), (5.2) for all values of $\nu > 0$ and $\Sigma_0 > 0$. We will show that the constructed solution will have the inner behavior of (5.4) and the outer behavior of (5.6).

Theorem 5.1. *Let $\Sigma_0 > 0$ be fixed. Let us note $c_\nu = 1 + \nu(n+1)/\alpha$. Given $\nu > 0$ there exists a solution $(\Sigma_\nu, U_\nu, \Theta_\nu)$ of (5.1), (5.2) defined for $\xi \in (0, \infty)$ and satisfying the properties:*

(i) *It achieves the initial data*

$$(5.7) \quad \lim_{\xi \rightarrow 0} \begin{pmatrix} \Sigma(\xi) \\ U(\xi) \\ \Theta(\xi) \end{pmatrix} = \begin{pmatrix} \Sigma_0 \\ U_0 \\ \Theta_0 \end{pmatrix},$$

where Σ_0 as in (5.2) and U_0, Θ_0 are defined via

$$(5.8) \quad \begin{aligned} U_0 \Sigma_0 &= c_\nu \\ \Theta_0 &= \frac{n+1}{\alpha} \log U_0 - \frac{1}{\alpha} \log c_\nu, \end{aligned}$$

(ii) *As $\xi \rightarrow \infty$ it has the limiting behavior*

$$(5.9) \quad \begin{aligned} U(\xi) &= \frac{1}{\xi} + o\left(\frac{1}{\xi}\right) \\ \Sigma(\xi) &= \xi + o(\xi) \\ \Theta(\xi) &= -\frac{n+1}{\alpha} \log \xi + o(1) \end{aligned}$$

(iii) The solution has the regularity $U, \Theta \in C^1[0, \infty), \Sigma \in C^2([0, \infty))$. It satisfies

$$(5.10) \quad \frac{d\Sigma}{d\xi}(0) = \frac{dU}{d\xi}(0) = \frac{d\Theta}{d\xi}(0) = 0,$$

and has the Taylor expansion as $\xi \rightarrow 0$,

$$(5.11) \quad \begin{aligned} U(\xi) &= U_0 + o(\xi) \\ \Sigma(\xi) &= \Sigma_0 + \frac{1}{2}U_0\xi^2 + o(\xi^2) \\ \Theta(\xi) &= \Theta_0 + o(\xi), \end{aligned}$$

where as usual $\lim_{\xi \rightarrow 0} \frac{1}{\xi}o(\xi) = 0$ (but the rate may degenerate as ν tends to 0).

Proof. Step 1. Motivated by the special solution (5.6) we introduce a change of variables in two steps:

$$(5.12) \quad \begin{aligned} U(\xi) &= \frac{1}{\xi}\bar{u}(\xi) &= \frac{1}{\xi}u(\log \xi) \\ \Sigma(\xi) &= \xi\bar{\sigma}(\xi) &= \xi\sigma(\log \xi) \\ \Theta(\xi) &= -\frac{n+1}{\alpha}\log \xi + \bar{\theta}(\xi) = -\frac{n+1}{\alpha}\log \xi + \theta(\log \xi) \end{aligned}$$

Indeed, we easily check that $(\bar{u}, \bar{\sigma}, \bar{\theta})(\xi)$ satisfies the system of equations

$$(5.13) \quad \begin{aligned} \xi \bar{\sigma}' &= \bar{u} - \bar{\sigma} \\ \nu \xi \bar{\theta}' &= \bar{\sigma} \bar{u} - 1 \\ \bar{\sigma} &= e^{-\alpha \bar{\theta}} \bar{u}^n. \end{aligned}$$

In the second step, we introduce in (5.13) the change of independent variable $\eta = \log \xi$ and derive that $(u, \sigma, \theta)(\eta)$ satisfy

$$(5.14) \quad \begin{aligned} \frac{d\sigma}{d\eta} &= u - \sigma \\ \nu \frac{d\theta}{d\eta} &= \sigma u - 1 \\ \sigma &= e^{-\alpha \theta} u^n. \end{aligned}$$

The system (5.14) is far simpler than the original (5.1) in that it is autonomous and non singular.

Step 2. We next consider (5.14) and perform a further simplification, via the change of dependent variables

$$(5.15) \quad \begin{aligned} a &:= \frac{1}{\sigma} \\ b &:= \frac{1}{\sigma^{1+\frac{1}{n}} e^{\frac{\alpha}{n}\theta}} = \frac{1}{\sigma u}. \end{aligned}$$

Note that $u = \frac{a}{b}$. We now compute

$$\frac{da}{d\eta} = -\frac{1}{\sigma^2} \frac{d\sigma}{d\eta} = -\frac{1}{\sigma^2} \left(\sigma^{\frac{1}{n}} e^{\frac{\alpha}{n}\theta} - \sigma \right) = a - \frac{a^3}{b}$$

and

$$\begin{aligned}
\frac{db}{d\eta} &= -\left(1 + \frac{1}{n}\right)b \frac{1}{\sigma} \frac{d\sigma}{d\eta} - \frac{\alpha}{n}b \frac{d\theta}{d\eta} \\
&= -\frac{n+1}{n}b \frac{1}{\sigma} \left(\frac{1}{\sigma b} - \sigma \right) - \frac{\alpha}{n}b \left(\frac{1}{b} - 1 \right) \\
&= \frac{\alpha}{n} \left(\left(1 + \nu \frac{n+1}{\alpha}\right)b - 1 - \frac{n+1}{\alpha} \nu a^2 \right)
\end{aligned}$$

In summary, we conclude that $(a, b)(\eta)$ satisfies the autonomous system of ordinary differential equations

$$(5.16) \quad \frac{d}{d\eta} \begin{pmatrix} a \\ b \end{pmatrix} = \begin{pmatrix} a \left(1 - \frac{a^2}{b}\right) \\ \frac{\alpha}{n} \left(c_\nu b - 1 - \frac{n+1}{\alpha} \nu a^2 \right) \end{pmatrix} =: F(a, b)$$

where

$$(5.17) \quad c_\nu := \left(1 + \nu \frac{n+1}{\alpha}\right) > 1.$$

There are two advantages in (5.16) relative to (5.14):

- (i) (5.16) is expressed via only two independent variables (a, b) .
- (ii) The equilibrium at infinity in (5.14) is pulled at the axis for (5.16) via the transformation (5.15).

Step 3. We perform a phase space analysis of (5.16) and establish the existence of a heteroclinic connection. We show:

Proposition 5.2. *Consider the autonomous planar system of differential equations (5.16) with c_ν defined by (5.17). For any $\nu > 0$ the system has the following properties:*

- *F has two equilibria $P = (0, 1/c_\nu)$, $Q = (1, 1)$ in the first quadrant. Both P and Q are hyperbolic points, P is a repelling node while Q is a saddle point.*
- *There exists a heteroclinic orbit connecting P to Q .*

Proof of Proposition 5.2.

- (a) The system (5.16) has the special solution

$$\begin{aligned}
a(\eta) &= 0 \\
b(\eta) &\text{ solves the differential equation } \frac{db}{d\eta} = \frac{\alpha}{n} (c_\nu b - 1)
\end{aligned}$$

This solution splits the phase portrait into the left and right plane and acts as a barrier from crossing from the one side to the other.

- (b) The equilibria of (5.16) are computed by solving

$$\begin{aligned}
a \left(1 - \frac{a^2}{b}\right) &= 0 \\
c_\nu b - 1 - \frac{n+1}{\alpha} \nu a^2 &= 0
\end{aligned}$$

and they are $P = (0, \frac{1}{c_\nu})$ and $Q = (1, 1)$ and $R = (-1, 1)$. Focusing on the behavior in the first quadrant we neglect the equilibrium R .

- (c) A computation shows

$$(5.18) \quad \nabla F(a, b) = \begin{pmatrix} 1 - \frac{3a^2}{b} & \frac{a^3}{b^2} \\ -2\frac{n+1}{n}a & \frac{\alpha}{n\nu}c_\nu \end{pmatrix}$$

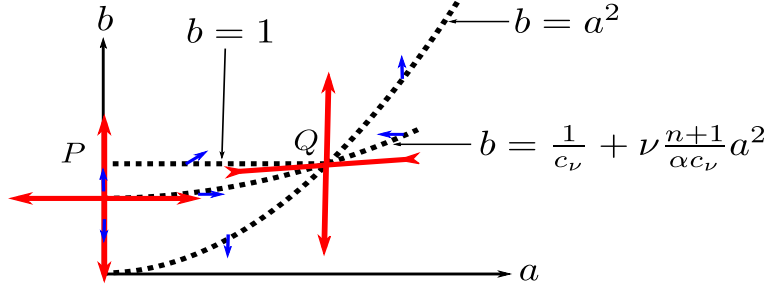


FIGURE 3. Phase diagram of System (5.16)

At the equilibrium P we have

$$\nabla F(0, \frac{1}{c_\nu}) = \begin{pmatrix} 1 & 0 \\ 0 & \frac{\alpha}{n\nu}c_\nu \end{pmatrix}$$

and we have eigenvalues $\lambda_1 = 1$ with eigenvector $r_1 = (1, 0)^T$, and $\lambda_2 = \frac{\alpha}{n\nu}c_\nu > 0$ with eigenvector $r_2 = (0, 1)^T$. In view of (5.17), we have $\lambda_2 > 1$. The local behavior of solutions of (5.16) around the equilibrium P is that of a repelling node. Standard phase plane theory for second order systems (*e.g.* [9]) states that there is a small neighborhood of the equilibrium P such that for any given solution $(a(\eta), b(\eta))$ of (5.16) there are constants κ_1, κ_2 such that

$$(5.19) \quad \begin{pmatrix} a(\eta) \\ b(\eta) \end{pmatrix} = \begin{pmatrix} 0 \\ \frac{1}{c_\nu} \end{pmatrix} + \kappa_1 \begin{pmatrix} 1 \\ 0 \end{pmatrix} e^{\lambda_1 \eta} + \kappa_2 \begin{pmatrix} 0 \\ 1 \end{pmatrix} e^{\lambda_2 \eta} + \text{higher order terms}$$

as $\eta \rightarrow -\infty$.

(d) At the point $Q = (1, 1)$ equation (5.18) gives

$$\nabla F(1, 1) = \begin{pmatrix} -2 & 1 \\ -2\frac{n+1}{n} & \frac{\alpha}{n\nu}c_\nu \end{pmatrix}$$

The eigenvalues λ_\pm , computed by

$$(5.20) \quad \lambda_\pm = \frac{(\frac{\alpha}{n\nu}c_\nu - 2) \pm \sqrt{(\frac{\alpha}{n\nu}c_\nu - 2)^2 + 8\frac{\alpha}{n\nu}}}{2},$$

are $\lambda_- < 0$ with eigenvector $r_- = (1, 2 + \lambda_-)^T$ and $\lambda_+ > 0$ with eigenvector $r_+ = (1, 2 + \lambda_+)^T$. Q is a saddle point.

(e) Consider the region \mathcal{R} bounded by the curves

- l_0 is the b -axis defined by the equation $a = 0$
- l_1 is the horizontal line $b - 1 = 0$
- l_2 is the parabola $b - a^2 = 0$

The region \mathcal{R} is expressed as

$$\mathcal{R} = \{(a, b) : a^2 \leq b \leq 1, 0 \leq a \leq 1\}$$

see Figure 3. We will show that \mathcal{R} is negatively invariant.

Indeed, the flow of (5.16) is parallel to l_0 as indicated in (b). On the horizontal line $l_1 \cap \mathcal{R}$ the system (5.16) gives

$$\frac{da}{d\eta} = a(1 - a^2) > 0, \quad \frac{db}{d\eta} = \frac{n+1}{n}(1 - a^2) > 0.$$

On the curve $l_2 \cap \mathcal{R}$ the system (5.16) gives

$$\frac{da}{d\eta} = 0, \quad \frac{db}{d\eta} = \frac{\alpha}{\nu n}(a^2 - 1) < 0.$$

Therefore \mathcal{R} is negatively invariant.

- (f) For completeness we also show that the vector r_- associated to the eigenvalue λ_- at Q points towards the interior of the region \mathcal{R} . Recall that Q is the upper right corner of the region \mathcal{R} and that

$$\begin{aligned} \text{the tangent vector to } l_1 \text{ is } \tau_1 &= (1, 0)^T \\ \text{the tangent vector to } l_2 \text{ at } Q &= (1, 1) \text{ is } \tau_2 = (1, 2)^T \\ \text{the eigenvector } r_- &= (1, 2 + \lambda_-)^T. \end{aligned}$$

We will show that

$$(5.21) \quad 0 < 2 + \lambda_- < 2, \quad \forall \nu > 0.$$

This then implies that the vector $-(r_-)$ when placed at the corner Q points strictly towards the interior of \mathcal{R} .

To show (5.21) recall that $\lambda_- < 0$ and use (5.20) and (5.17) to rewrite

$$2(\lambda_- + 2) = \left(\frac{\alpha}{n\nu}c_\nu + 2\right) - \sqrt{I}$$

where

$$\begin{aligned} I &:= \left(\frac{\alpha}{n\nu}c_\nu - 2\right)^2 + 8\frac{\alpha}{n\nu} \\ &= \left(\frac{\alpha}{n\nu}c_\nu\right)^2 + 4 + 4\frac{\alpha}{n\nu} - 4\frac{n+1}{n} \\ &< \left(\frac{\alpha}{n\nu}c_\nu\right)^2 + 4 + 4\frac{\alpha}{n\nu} \\ &< \left(\frac{\alpha}{n\nu}c_\nu + 2\right)^2 \end{aligned}$$

This shows $\lambda_- + 2 > 0$ and concludes (5.21).

- (g) It is easy to check that there can be no closed limit cycle in \mathcal{R} because in that region

$$\frac{da}{d\eta} = \frac{a}{b}(b - a^2) > 0.$$

The Poincaré-Bendixson theorem implies that there exists a heteroclinic orbit joining $(0, \frac{1}{c_\nu})$ and $(1, 1)$ which emanates along the direction of the stable manifold at $(1, 1)$ and progresses backwards in time towards the node at $(0, \frac{1}{c_\nu})$. \square

Step 4. We turn now to defining the solution of (5.1), (5.2). Let $(A(\eta), B(\eta))$ stand for a parametrization of the heteroclinic orbit. In view of (5.19) and the fact that $\lambda_2 > \lambda_1 = 1$, there exists a constant κ_1 such that

$$(5.22) \quad e^{-\eta} \left(\begin{pmatrix} A(\eta) \\ B(\eta) \end{pmatrix} - \begin{pmatrix} 0 \\ \frac{1}{c_\nu} \end{pmatrix} \right) \rightarrow \kappa_1 \begin{pmatrix} 1 \\ 0 \end{pmatrix} \quad \text{as } \eta \rightarrow -\infty,$$

Due to the fact that the vertical axis is a trajectory of its own and thus distinct from the trajectory we are considering, and due to the form of the phase portrait we can assert that $\kappa_1 > 0$.

For any $\eta_0 \in \mathbb{R}$ the function $(A(\eta + \eta_0), B(\eta + \eta_0))$ offers an alternative parametrization of the same heteroclinic orbit. Applying (5.22) to this parametrization yields

$$(5.23) \quad e^{-\eta} \left(\begin{pmatrix} A(\eta + \eta_0) \\ B(\eta + \eta_0) \end{pmatrix} - \begin{pmatrix} 0 \\ \frac{1}{c_\nu} \end{pmatrix} \right) \rightarrow \kappa_1 e^{\eta_0} \begin{pmatrix} 1 \\ 0 \end{pmatrix} \quad \text{as } \eta \rightarrow -\infty.$$

Choose η_0 such that $\kappa_1 \eta_0 = \frac{1}{\Sigma_0}$ and let $(a(\eta), b(\eta))$ denote the corresponding parametrization of the heteroclinic :

$$\begin{pmatrix} a(\eta) \\ b(\eta) \end{pmatrix} := \begin{pmatrix} A(\eta + \eta_0) \\ B(\eta + \eta_0) \end{pmatrix}$$

The selected parametrization satisfies as $\eta \rightarrow -\infty$

$$\begin{aligned}
(5.24) \quad a(\eta) &= \frac{1}{\Sigma_0} e^\eta + o(1) e^\eta \\
b(\eta) &= \frac{1}{c_\nu} + o(1) e^\eta \\
\sigma(\eta) &= \frac{1}{a(\eta)} = \frac{\Sigma_0 e^{-\eta}}{1 + o(1)} = \Sigma_0 e^{-\eta} (1 + o(1))
\end{aligned}$$

where as usual $o(1) \rightarrow 0$ as $\eta \rightarrow -\infty$.

Recalling the changes of variables (5.12) and (5.15) we define

$$\begin{aligned}
(5.25) \quad U(\xi) &= \frac{1}{\xi} u(\log \xi) &= \frac{1}{\xi} \left(\frac{a}{b} \right) (\log \xi) \\
\Sigma(\xi) &= \xi \sigma(\log \xi) &= \xi \left(\frac{1}{a} \right) (\log \xi) \\
\Theta(\xi) &= -\frac{n+1}{\alpha} \log \xi + \theta(\log \xi) = -\frac{n+1}{\alpha} \log \xi + \frac{n+1}{\alpha} (\log a) (\log \xi) - \frac{n}{\alpha} (\log b) (\log \xi).
\end{aligned}$$

The function (5.25) clearly satisfies the system (5.1) and, since $(a(\eta), b(\eta)) \rightarrow (1, 1)$ as $\eta \rightarrow \infty$, it satisfies

$$\begin{aligned}
U(\xi) &= \frac{1}{\xi} (1 + o(1)) \\
\Sigma(\xi) &= \xi (1 + o(1)) \\
\Theta(\xi) &= -\frac{n+1}{\alpha} \log \xi + o(1)
\end{aligned}$$

as ξ goes to infinity, which shows (5.9).

Step 5. In the last step, we study the behavior near the (apparent) singular point at $\xi = 0$ and prove that the solution is in fact regular there and satisfies (5.7), (5.10) and (5.11).

Clearly (5.24) and (5.25)₂ imply that $\Sigma(\xi) \rightarrow \Sigma_0$ as $\xi \rightarrow 0$. Let U_0 and Θ_0 be defined by (5.8). Since $u(\eta) = \frac{a}{b}(\eta)$, (5.24) gives

$$(5.26) \quad u(\eta) = \frac{a}{b}(\eta) = \frac{c_\nu}{\Sigma_0} e^\eta + o(1) e^\eta = U_0 e^\eta + o(1) e^\eta.$$

Now (5.25), (5.24), (5.26), (5.8) imply

$$\begin{aligned}
\Theta(\xi) &= -\frac{n+1}{\alpha} \log \xi + \frac{n+1}{\alpha} \log \left(\xi \frac{1}{\Sigma_0} (1 + o(1)) \right) - \frac{n}{\alpha} \log \left(\frac{1}{c_\nu} + o(1) \right) \\
&\rightarrow \frac{n+1}{\alpha} \log \left(\frac{1}{\Sigma_0} \right) - \frac{n}{\alpha} \log \left(\frac{1}{c_\nu} \right) = \Theta_0 \quad \text{as } \xi \rightarrow 0.
\end{aligned}$$

and together with (5.26) and (5.25) provide (5.7).

Observe now that

$$\frac{dU}{d\xi}(\xi) = \frac{1}{\xi^2} \left(\frac{du}{d\eta} - u \right) (\log \xi).$$

24

Using (5.16), (5.24) and (5.26), we obtain

$$\begin{aligned}
\frac{du}{d\eta} - u &= \frac{1}{b} \frac{da}{d\eta} - \frac{a}{b^2} \frac{db}{d\eta} - \frac{a}{b} \\
&= \frac{1}{b} a \left(1 - \frac{a^2}{b}\right) - \frac{a}{b} - \frac{a}{b^2} \left[\frac{\alpha}{\nu n} (c_\nu b - 1) - \frac{n+1}{n} a^2 \right] \\
&= \frac{1}{n} u^3 b - u \frac{\alpha}{\nu n} \frac{c_\nu}{b} \left(b - \frac{1}{c_\nu}\right) \\
&= \frac{1}{n} \frac{U_0^3}{c_\nu} e^{3\eta} (1 + o(1)) - \frac{\alpha}{\nu n} U_0 o(1) e^{2\eta} \quad \text{as } \eta \rightarrow -\infty
\end{aligned}$$

and thus

$$(5.27) \quad \left| \frac{dU}{d\xi}(\xi) \right| \leq o(1) \quad \text{as } \xi \rightarrow 0.$$

Since $U \in C[0, 1] \cap C^1(0, 1)$ the mean value theorem implies

$$\left| \frac{U(\xi) - U_0}{\xi} \right| = |U'(\xi^*)| \quad \text{for some } \xi^* \in (0, \xi),$$

and (5.27) implies $U'(0)$ exists and $U'(0) = 0$. We conclude that $U \in C^1[0, \infty)$ has the Taylor expansion (5.11)₁. In turn, $\Sigma \in C^2[0, \infty)$, $\Sigma'(0) = 0$, $\Sigma''(0) = \frac{1}{2}U_0$ and Σ achieves the Taylor expansion (5.11)₂.

Turning to Θ , observe that by (5.24) and (5.25)₃

$$\begin{aligned}
\theta(\eta) &= \frac{n+1}{\alpha} \log a(\eta) - \frac{n}{\alpha} \log b(\eta) \\
&= \frac{n+1}{\alpha} \log \left(\frac{1}{\Sigma_0} e^\eta (1 + o(1)) \right) - \frac{n}{\alpha} \log \left(\frac{1}{c_\nu} (1 + o(1) e^\eta) \right) \\
&= \frac{n+1}{\alpha} \log \frac{1}{\Sigma_0} - \frac{n}{\alpha} \log \frac{1}{c_\nu} + \frac{n+1}{\alpha} \log e^\eta + \frac{n+1}{\alpha} \log(1 + o(1)) - \frac{n}{\alpha} \log(1 + o(1) e^\eta) \\
&= \Theta_0 + \frac{n+1}{\alpha} \eta + \frac{n+1}{\alpha} \log(1 + o(1)) - \frac{n}{\alpha} \log(1 + o(1)), \quad \text{as } \eta \rightarrow -\infty,
\end{aligned}$$

while

$$\begin{aligned}
\Theta(\xi) &= -\frac{n+1}{\alpha} \log \xi + \theta(\log \xi) \\
&= \Theta_0 + o(1) \quad \text{as } \xi \rightarrow 0.
\end{aligned}$$

In addition,

$$\Theta'(\xi) = -\frac{n+1}{\alpha} \frac{1}{\xi} + \frac{1}{\xi} \frac{d\theta}{d\eta}(\log \xi)$$

combined with the formula

$$\begin{aligned}
\frac{d\theta}{d\eta} &= \frac{n+1}{\alpha} \frac{1}{a} \frac{da}{d\eta} - \frac{n}{\alpha} \frac{1}{b} \frac{db}{d\eta} \\
&= \frac{n+1}{\alpha} \left(1 - \frac{a^2}{b} \right) - \frac{1}{\nu} \left(c_\nu - \frac{1}{b} \right) + \frac{n+1}{\alpha} \frac{a^2}{b} \\
&= \frac{n+1}{\alpha} - \frac{1}{\nu} \frac{c_\nu}{b} \left(b - \frac{1}{c_\nu} \right)
\end{aligned}$$

gives

$$\begin{aligned}
\Theta'(\xi) &= -\frac{1}{\xi} \left(\frac{c_\nu}{b} \left(b - \frac{1}{c_\nu} \right) \right) (\log \xi) \\
&= -\frac{1}{\xi} \frac{c_\nu}{b} (\log \xi) o(1) \xi \\
&= o(1) \rightarrow 0 \quad \text{as } \xi \rightarrow 0.
\end{aligned}$$

This shows $\Theta \in C^1[0, \infty)$ has the Taylor expansion (5.11)₃ at the origin. □

6. LOCALIZATION - PART II

We are ready to state and prove the main result of the paper. This concerns the adiabatic case $\kappa = 0$ of system (2.1), taken now on the whole real line $(x, t) \in \mathbb{R} \times \mathbb{R}^+$ and expressed in terms of the variable $u = v_x$ in the form:

$$(6.1) \quad \begin{aligned} u_t &= \sigma_{xx} \\ \theta_t &= \sigma u \\ \sigma &= e^{-\alpha\theta} u^n. \end{aligned}$$

Our analysis is based on the transformations of section 4 and the self-similar solution constructed in section 5.

Theorem 6.1. *Let $\theta_0 > 0$ and $\Sigma_0 > 0$ be given. For any $\lambda > 0$, the system (6.1) admits a special class of solutions describing localization of the form:*

$$(6.2) \quad u(x, t) = \left(\frac{\alpha}{c_0}t + 1\right)^{\frac{\lambda}{\alpha}} U_\lambda \left(\sqrt{\lambda}x \left(\frac{\alpha}{c_0}t + 1\right)^{\frac{\lambda}{\alpha}} \right)$$

$$(6.3) \quad \sigma(x, t) = \sigma_s(t) \left(\frac{\alpha}{c_0}t + 1\right)^{-\frac{\lambda}{\alpha}} \Sigma_\lambda \left(\sqrt{\lambda}x \left(\frac{\alpha}{c_0}t + 1\right)^{\frac{\lambda}{\alpha}} \right)$$

$$(6.4) \quad \theta(x, t) = \left(1 + \lambda \frac{n+1}{\alpha}\right) \theta_s(t) - \lambda \frac{n+1}{\alpha} \theta_0 + \Theta_\lambda \left(\sqrt{\lambda}x \left(\frac{\alpha}{c_0}t + 1\right)^{\frac{\lambda}{\alpha}} \right)$$

where σ_s, θ_s are the uniform shear solutions in (2.10), $c_0 = e^{\alpha\theta_0}$, while $(U_\lambda, \Sigma_\lambda, \Theta_\lambda)(\xi)$ is an even function defined on \mathbb{R} , which solves the initial value problem (5.1), (5.2) with $\nu = \lambda > 0$ for $\xi \in [0, \infty)$.

Remark 6.2.

- (i) Because $\left(\frac{\alpha}{c_0}t + 1\right)^{\frac{\lambda}{\alpha}}$ goes to infinity in time, the level curves of

$$\xi(x, t) = \sqrt{\lambda}x \left(\frac{\alpha}{c_0}t + 1\right)^{\frac{\lambda}{\alpha}}$$

accumulate along the $\{x = 0\}$ axis in the (x, t) plane. The functions (6.2), (6.3), (6.4) thus describe a localizing solution where the flow tends to concentrate around $x = 0$ as the time proceeds.

- (ii) The solution (6.2), (6.3), (6.4) is defined on $\mathbb{R} \times \mathbb{R}^+$ and emanates from initial data

$$(6.5) \quad \begin{aligned} u(x, 0) &= U_\lambda(\sqrt{\lambda}x) \\ \sigma(x, 0) &= \sigma_s(0) \Sigma_\lambda(\sqrt{\lambda}x) \\ \theta(x, 0) &= \theta_s(0) + \Theta_\lambda(\sqrt{\lambda}x). \end{aligned}$$

The initial data depend on two parameters: The parameter λ which can be thought as a length scale in initial data, and Σ_0 in (5.2) which describes the amplitude of the initial perturbation.

- (iii) This parametric family of solutions is valid for any $\lambda > 0$. If λ is large then the length scale of the initial perturbation is short while the growth in time and the rate of localization for the solution become fast.

Proof. We introduce the changes of variables (4.1) and the stationary variant of (4.7), which once combined together reads

$$(6.6) \quad \begin{aligned} u(x, t) &= \frac{1}{r(\tau(t))} \bar{U}\left(\frac{x}{r(\tau(t))}\right) \\ \sigma(x, t) &= \sigma_s(t) r(\tau(t)) \bar{\Sigma}\left(\frac{x}{r(\tau(t))}\right) \\ \theta(x, t) &= \theta_s(t) - \frac{n+1}{\alpha} \log r(\tau(t)) + \bar{\Theta}\left(\frac{x}{r(\tau(t))}\right). \end{aligned}$$

We select $r(\tau) = e^{-\lambda\tau}$ with $\lambda > 0$. According to the analysis in section 4.3 the function $(\bar{U}, \bar{\Sigma}, \bar{\Theta})(\xi)$ is sought as a solution of (4.10) defined on the interval $(-\infty, \infty)$.

The desired $(\bar{U}, \bar{\Sigma}, \bar{\Theta})(\xi)$ is constructed as follows. First, observe the relation between the system (4.10) and the system (5.1). Let Σ_0 be fixed, and let $(U_\lambda, \Sigma_\lambda, \Theta_\lambda)(\xi)$ be the solution of (5.1) with $\nu = \lambda$ and (5.2), defined for $\xi \in [0, \infty)$. This solution is well defined by Theorem 5.1. Using a direct computation, the smoothness properties in (iii) of Theorem 5.1, and (5.5) we conclude that

(a) The function $(\bar{U}, \bar{\Sigma}, \bar{\Theta})$ defined by

$$(6.7) \quad \bar{U}(\xi) = U_\lambda(\sqrt{\lambda}\xi), \quad \bar{\Sigma}(\xi) = \Sigma_\lambda(\sqrt{\lambda}\xi), \quad \bar{\Theta}(\xi) = \Theta_\lambda(\sqrt{\lambda}\xi)$$

satisfies (4.10) on \mathbb{R}^+ and the condition $\bar{\Sigma}(0) = \Sigma_0$.

(b) If we extend $(\bar{U}, \bar{\Sigma}, \bar{\Theta})$ on $(-\infty, 0)$ by setting $(\bar{U}, \bar{\Sigma}, \bar{\Theta})(-\xi) = (\bar{U}, \bar{\Sigma}, \bar{\Theta})(\xi)$ for $\xi < 0$, the resulting function $\bar{U}, \bar{\Theta} \in C^1(\mathbb{R})$, $\bar{\Sigma} \in C^2(\mathbb{R})$ is a solution of (4.10) defined on the whole real line that is even.

Noting that

$$r(\tau(t)) = e^{-\lambda\tau(t)} = \left(\frac{\alpha}{c_0}t + 1\right)^{-\frac{\lambda}{\alpha}}$$

we combine (6.6) with (6.7) and (2.10) to arrive at (6.2), (6.3), (6.4). □

In Figure 4 the profiles of $u(x, t)$ and $\theta(x, t)$ in (6.2) and (6.4), respectively, are drawn at various instances of time from $t = 0$ to $t = 200$. To achieve these profiles, we construct numerically the heteroclinic orbit for (5.16) whose existence is justified in Proposition 5.2. The construction is simple, if one exploits the special properties of system (5.16), and proceeds as follows: Initial conditions (a_0, b_0) are selected close to the equilibrium $Q = (1, 1)$ inside the region \mathcal{R} and in the direction of the stable manifold of Q for the linearized problem. Then (5.16) is solved backward in time, using an ode solver, and since $P = (0, 1/c_\nu)$ is an unstable node (for the forward problem) the resulting orbit is a good approximation of the heteroclinic. For the integration of (5.16) we use an explicit Runge–Kutta predictor-corrector method of order (4,5) with adaptive time stepping. Then Σ_0 is selected by choosing an appropriate parametrisation η_0 following the construction in (5.23).

For the numerical runs the constitutive parameters are $n = 0.1$, $\alpha = 0.5$. The parameters related to the solution are $\theta_0 = 10$, $\lambda = 0.1$ while for the selected reparametrization of the heteroclinic orbit the value of $\Sigma_0 = 1.88$. Once the heteroclinic has been constructed, the profiles $U_\lambda, \Theta_\lambda$ are computed via the changes of variables (5.15) and (5.12). Finally, $u(x, t)$ and $\theta(x, t)$ are computed by (6.2), (6.4) respectively with $\theta_0 = 10$, and are presented in Fig 4.

The solution presented in Fig 4 evidently exhibits localisation as time increases: a coherent structure forms where the deformation localizes in a narrow band. In this self-similar solution there is no trace of the oscillations, captured by the higher order modes (3.22), that are everywhere present in solutions to the linearized problem (3.9) with $k = 0$. The nonlinearity suppresses the oscillations and a seamless coherent structure emerges.

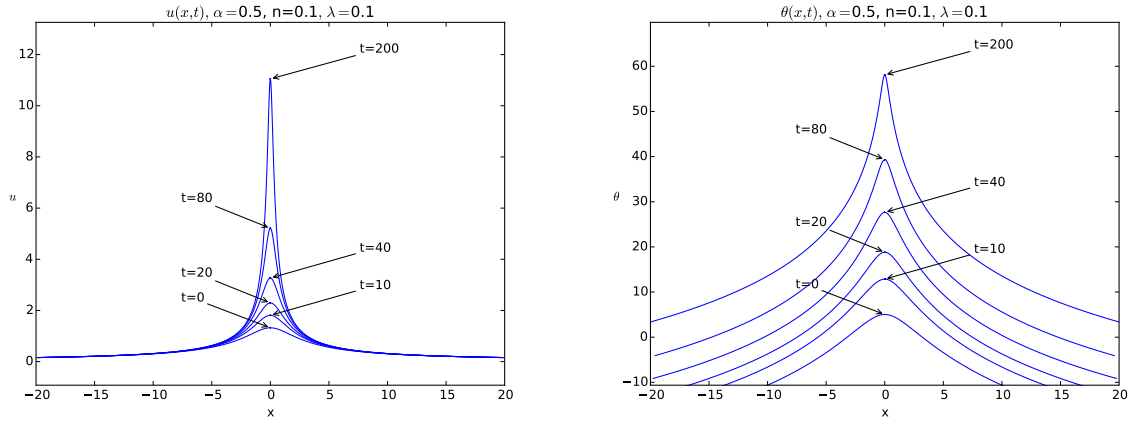


FIGURE 4. The solution $u(x, t)$, (6.2) and $\theta(x, t)$, (6.4).

REFERENCES

- [1] TH. BAXEVANIS, TH. KATSAOUNIS AND A.E. TZAVARAS, *Adaptive finite element computations of shear band formation* Math. Models Methods Applied Sciences **20** (2010), 423-448.
- [2] M.BERTSCH, L.A.PELETIER AND S.M.VERDUYN LUNEL, *The effect of temperature dependent viscosity on shear flow of incompressible fluids* SIAM J. Math. Anal., **22** (1991), 328-343.
- [3] R.J.CLIFTON, J.DUFFY, K.A.HARTLEY AND T.G.SHAWKI, *On critical conditions for shear band formation at high strain rates*, Scripta Met., **18** (1984), 443-448.
- [4] C.M.DAFERMOS AND L.HSIAO, *Adiabatic shearing of incompressible fluids with temperature dependent viscosity* Quart. Appl. Math., **41** (1983), 45 - 58.
- [5] J.A. DILELLIO AND W.E. OLMSTEAD, *Shear band formation due to a thermal flux inhomogeneity* SIAM J. Appl. Math., **57** (1997), 959-971.
- [6] D.J. ESTEP, S.M.V.LUNEL, AND R.D.WILLIAMS, *Analysis of shear layers in a fluid with temperature-dependent viscosity* Comp. Physics, **173** (2001), 17-60.
- [7] C. FRESSENCEAS AND A. MOLINARI, *Instability and localization of plastic flow in shear at high strain rates*, J Mech Phys Solids **35** (1987), pp. 185-211.
- [8] K.A.HARTLEY, J.DUFFY, AND R.J.HAWLEY, *Measurement of the temperature profile during shear band formation in steels deforming at high-strain rates* J. Mech. Physics Solids, **35** (1987), 283-301.
- [9] PH. HARTMAN, *Ordinary differential equations. Corrected reprint of the second (1982) edition* [Birkhäuser, Boston, MA]. Classics in Applied Mathematics, 38. SIAM, Philadelphia, PA, 2002.
- [10] TH. KATSAOUNIS AND A.E. TZAVARAS, *Effective equations for localization and shear band formation*, SIAM J. of Applied Math., **69**, no.6, (2009), pp.1618-1643.
- [11] TH. KATSAOUNIS AND A.E. TZAVARAS, *Localization and shear bands in high strain-rate plasticity*. In Nonlinear Conservation Laws and Applications , A. Bressan, G.-Q. Chen, M. Lewicka and D. Wang, eds; IMA Vol. Math. Appl., 153, Springer, New York, 2011, pp 365-378.
- [12] A.MOLINARI AND R.J.CLIFTON, *Analytical characterization of shear localization in thermoviscoplastic materials* J. Appl. Mech., **54** (1987), 806-812.
- [13] T.G. SHAWKI AND R.J. CLIFTON, *Shear band formation in thermal viscoplastic materials* Mech. Materials, **8**, (1989), 13-43.
- [14] A.M. TURING, *The chemical basis of morphogenesis* Phil. Trans. R. Soc. Lond. B, **237** (1952), 37-72.
- [15] A.E.TZAVARAS, *Effect of thermal softening in shearing of strain-rate dependent materials* Arch. Rational Mech. Analysis, **99** (1987), 349 - 374.
- [16] A.E.TZAVARAS, *Strain softening in viscoelasticity of the rate type* J. Integral Equations Appl., **3** (1991), 195-238.
- [17] A.E.TZAVARAS, *Nonlinear analysis techniques for shear band formation at high strain rates*. Appl. Mech. Reviews, **45** (1992), S82-S94.
- [18] J.W. WALTER, *Numerical experiments on adiabatic shear band in one space dimension*. Int. J. of Plasticity, **8** (1992), 657-693.

- [19] T.W.WRIGHT AND J.W.WALTER, *On stress collapse in adiabatic shear bands*. J. Mech. Phys. Solids, **35** (1988), 701-720.
- [20] T.W.WRIGHT AND H. OCKENDON, *A model for fully formed shear bands*. J. Mech. Phys. Solids, **40** (1992), 1217-1226.
- [21] T.W. WRIGHT, *The Physics and Mathematics of Shear Bands*, Cambridge University Press, 2002.
- [22] C.ZENER AND J.H.HOLLOMON, *Effect of strain rate upon plastic flow of steel* J. Appl. Physics, **15** (1944), 22-32.